SIZE REDUCTION AND PERFORMANCE ENHANCEMENT OF PLANAR ANTENNAS FOR L-BAND APPLICATION

A DISSERTATION

Submitted in partial fulfillment of the requirements for the award of the degree of

INTEGRATED DUAL DEGREE

(Bachelor of Technology & Master of Technology)

in

ELECTRONICS AND COMMUNICATION ENGINEERING

(With Specialization in Wireless Communication)

By

DAVINDER SINGH

DEPARTMENT OF ELECTRONICS AND COMPUTER ENGINEERING
INDIAN INSTITUTE OF TECHNOLOGY ROORKEE
ROORKEE - 247 667 (INDIA)

JUNE, 2012

CANDIDATE'S DECLARATION

I hereby declare that the work being presented in the dissertation entitled, "***Size reduction and performance enhancement of planar antennas for L-band application***" in partial fulfillment of the requirements for the award of the degree of ***Master of Technology*** in ***Electronics & Communication Engineering***, submitted in the Department of Electronics and Computer Engineering, Indian Institute of Technology Roorkee (India), is an authentic record of my own work carried out under the guidance of **Dr. Amalendu Patnaik**, Assistant Professor, Department of Electronics & Computer Engineering, Indian Institute of Technology Roorkee.

The matter embodied in this dissertation report has not been submitted for the award of any other degree elsewhere.

Date: 15 June, 2012

Place: IIT Roorkee

(Davinder Singh)

CERTIFICATE

This is to certify that the above statement made by the candidate is correct to the best of my knowledge.

Date:

Dr. Amalendu Patnaik 22/6/12

Place: IIT Roorkee

Assistant Professor

Department of Electronics and Computer Engineering

IIT Roorkee

ACKNOWLEDGEMENTS

It is difficult to overstate my gratitude to my supervisor, **Dr. Amalendu Patnaik**, Assistant Professor, Department of Electronics and Computer Engineering, Indian Institute of Technology Roorkee. Throughout my thesis-working period, he provided encouragement, sound advice, good teaching, good company, and lots of good ideas. I would have been lost without him. He is an inspiring professor, a great advisor and mostly a nice person.

It is a pleasure to thank **Dr. Padam Kumar**, Head of E&C Department, for facilitating the necessary requirements to carry out the work and for supporting at critical time during the thesis submission. I would also like to thank **Dr. D. Singh** and **Dr. N.P. Pathak**, for their encouragement and guidance in the RFand Microwave field during the entire tenure in IIT Roorkee.

I would also like to thank **Mr. Gaur**, **Mr.Rajaram**, for their valuable support and time to time guidance in technical issues, which was instrumental in making this dissertation work a success.

Finally, I would also like to thank all my friends, especially **Mr.Jagannath Malik**, for his support and valuable suggestions during this work. His knowledge in the field Metamaterial antenna was very helpful.

Above all, I thank my parents, my brother **Mr.Jitender Singh** and my friend **Miss. Richa Thakur** for their love, cooperation and encouragement which was a constant source of inspiration for me.

Last, but not the least, I thank God for his blessings.

(Davinder Singh)

ABSTRACT

High performance, compact size and low cost are the basic requirements of modern microwave communication systems. Various technologies have been developed to fulfill these requirements such as Substrate Integrated Waveguides (SIWs), Photonic Band Gap Structures (PBG), Defected Ground Structures (DGS), Electromagnetic Metamaterial structures and so on. Among these, Metamaterials are relatively new and the potential applications of these special classes of materials have drawn much attention in last few decades. Metamaterials firstly came into existence when V. G. Veselago introduced the concept of Left-Handed (LH) materials, materials which have Negative Refractive Index because of negative Permittivity and Permeability. These materials are not naturally occurring so a lot research is done to design and simulate such metamaterials which can be used for number of applications like thin resonators, filters and antennas. In antennas these materials are used to enhance its performance. It increases Directivity, Gain Radiated Power and reduces size to enhance the antenna performance.

As of today world, size reduction in antenna have gained much of interest as to decrease the sizes of communicating devices like mobile and remote sensing etc.In this dissertation, basic theory of metamaterial structures has been studied. A literature survey has been done to explore the application of Metamaterials to microstrip patch antennas.Thereafter microstrip patch antenna for L-band (1.28 GHz) was designed. To obtain size reduction Modified Split Ring Resonator (SRR) metamaterial structure was used to make various metamaterial antennas with the size reduction of about 80 percent as of microstrip patch antenna of same frequency.

All the designs were made with CST.

List of Figures

Contents

Chapter 1
Introduction

In this chapter introduction to metamaterial and microstrip patch antenna is briefly discussed as to familiarize with the basics concepts of the dissertation work. In the first part, a brief introduction to Metamaterials is given which includes the definition of the metamaterial, the early theory to the negative index of refraction and the structure that shows the left-handed properties. In second part, brief introduction to microstrip patch antenna is given. Then follows the objective and scope of the dissertation work which reflects the overall project's content.

1.1 Introduction to Metamaterials

Metamaterials (MTM) are artificial effectively homogenous structures with unusual electromagnetic properties which are not readily available in nature. An effectively homogenous structure has structural average cell size much smaller than the guided wavelength which ensures the dominance of refractive phenomenon over scattering/diffraction phenomenon when wave propagates inside the metamaterial. These materials usually gain their properties from structure rather than their composition [1, 2].

These unusual properties can be either negative permittivity or negative permeability and if both of them are negative at same frequency then material have negative Refractive Index for an isotropic medium. These Metamaterials are called as Left Handed Metamaterials (LHM) because Electric Field, Magnetic Field and Wave vector form Left Handed System LH materials as the consequence of their double negative parameters are characterized by anti parallel phase and group velocities or negative refractive index (NRI).

Refractive Index is related to Permittivity (ε) and permeability (μ) as

$$n=\pm\sqrt{\mu\epsilon} \qquad (1.1)$$

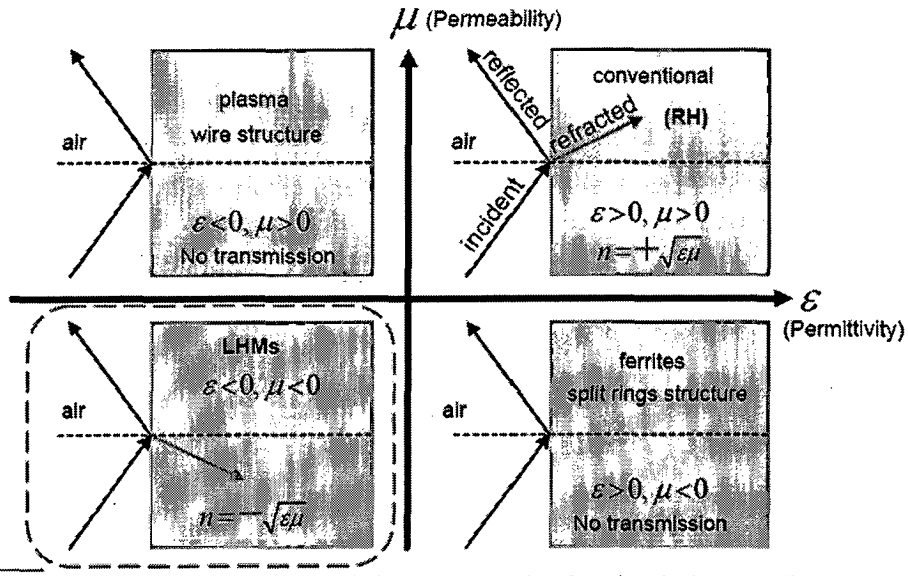

Figure 1.1: Permittivity-permeability (ε-μ) and refractive index (n) diagram [1]

According to this equation we get Negative Refractive Index for negative permittivity and permeability.

The negative permittivity is easily obtained by an array of metallic wires and was theorized in 1996. It was shown that the structure is having a plasma frequency in the microwave regime. Because of its low plasma frequency, this structure can produce an effective negative permittivity at microwave frequencies while suffering relatively small losses. J.B. Pendry also theorized the structure with negative permeability which was established in 1999 with split ring resonator (SRR) structure [3]. The first negative index medium was developed when both of these structures were combined and it was shown that the negative index of refraction exists in the region where both the real parts of the electric permittivity and magnetic permeability were simultaneously negative, typically in a structure composed of SRRs and strip wires.

Examples of Metamaterials are single negative materials (SNG) like ϵ_{eff} negative(ENG) which have effective negative permittivity and μ eff negative (MNG) which have effective negative permeability, and double negative materials

(DNG) realized by placing periodic structures that alter the material parameters. Split-ring resonators, metal-wire strips and complementary split-ring resonators are currently used to periodically embed the host medium to obtain 'Metamaterials'. The back-ward couplers [1, 4], phase compensation resulting in electrically small resonators[5], sub-wavelength waveguides with lateral dimensions below diffraction limits [6], enhanced focusing [7], Cerenkov radiation, Doppler effect, photon tunneling, and backward wave antennas [8], are some examples of applications and properties studied so far.

Metamaterials are used to enhance or increase the performance of antennas. Applying it to increase performance of antennas has garnered much interest. Demonstrations have shown that Metamaterials could enhance the radiated power of an antenna [1, 9]. Materials which can attain negative magnetic permeability could possibly allow for properties such as an electrically small antenna size, high directivity, and tunable operational frequency, including an array system. Metamaterial based antennas can demonstrate improved efficiency-bandwidth performance [9]. Antennas employing Metamaterials offer the revolutionary potential of overcoming restrictive efficiency-bandwidth limitations for natural or conventionally constructed electrically small antennas. Metamaterial antennas if successful would allow smaller antenna elements that cover a wider frequency range thus making better use of available space for small platforms or spaces [10]. Metamaterials employed in the ground planes surrounding antennas offers improved isolation between radio frequency or microwave channels of (multiple-input multiple-output) (MIMO) antenna arrays. Metamaterial high-impedance ground planes can also be used to improve the radiation efficiency, and axial radio performance of low-profile antennas located close to the ground plane surface. They have also been used to increase the beam scanning range by using both the forward and backward waves in leaky wave antennas. Various metamaterial antenna systems can be employed to support surveillance sensors, communication links, navigation systems, command and control systems.

Metamaterial are either volumetric or planar. During the dissertation work planar metamaterial was used. So in the next section planar metamaterial are discussed briefly.

1.1.1. Planar Metamaterial

The planar version of a metamaterial can be treated as a transmission line. Here we effectively apply the circuit approach based on the equivalent circuit of the transmission line consisting of lumped elements. This circuit shown in Fig. 1.2 consists of series impedance Z and parallel admittance Y and represents the element of the wavelength λ in order to form a unit cell.

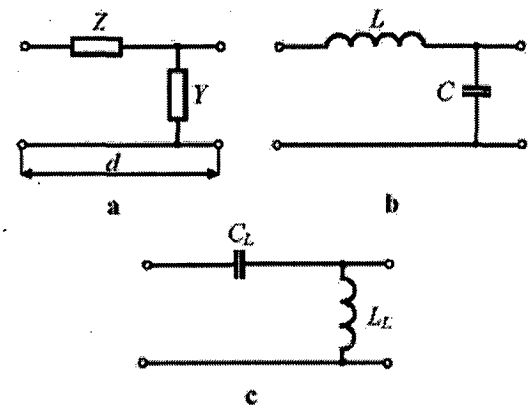

Figure1.2: The equivalent circuit of the general transmission lines (a) the standard *L-C* line (b) *C-L* left-handed line (c) Dual case.

Characteristic impedance of this transmission line is

$$Z_0 = \sqrt{\frac{Z}{Y}} \qquad (1.2)$$

The propagation constant $Y = \alpha + j\beta$ is

$$\gamma = \pm\sqrt{ZY} \qquad (1.3)$$

for the wave propagating in the positive z direction described by exp(-γz) we take + in (1.3), while the sign – in (1.3) represents the wave propagating in the negative z

direction. In next text we assume the positive sign. α and β are attenuation and phase constants. The phase velocity v_p is

$$v_p = \frac{\omega}{\beta} \tag{1.4}$$

and the group velocity v_g is

$$v_g = \frac{1}{\frac{\partial \beta}{\partial \omega}} \tag{1.5}$$

The standard lossless line has $Z=j\omega L$, $Y=j\omega C$ as shown in Fig. 1.2 b so from (1.2-1.5)

$$Z_0 = \sqrt{\frac{L}{C}} \tag{1.6}$$

$$\gamma = j\beta = j\omega\sqrt{LC} \tag{1.7}$$

$$v_p = \frac{1}{\sqrt{LC}} \tag{1.8}$$

$$v_g = \frac{1}{\sqrt{LC}} \tag{1.9}$$

This corresponds to the propagation of the standard TEM forward wave along the line. Both velocities v_p and v_g are positive. Now let us consider the dual case with the corresponding equivalent circuit shown in Fig. 1.2 c where the positions of the capacitance and inductance have been exchanged. In this way we have changed the original *L-C* low-pass structure into the *C-L* high-pass structure. The latter lines are denoted as left handed [11] and represent the planar version of a metamaterial. Now for the lossless line we have $\alpha = 0$, $Z = 1 / (j\omega C_L)$ *and* $Y = 1 / (j\omega L_L)$. Consequently

$$Z_0 = \sqrt{\frac{L_L}{C_L}} \tag{1.10}$$

$$\gamma = j\beta = -j\frac{1}{\omega\sqrt{L_L C_L}} \tag{1.11}$$

$$v_p = -\omega^2\sqrt{L_L C_L} \tag{1.12}$$

$$v_p = \omega^2 \sqrt{L_L C_L} \qquad (1.13)$$

There are different signs in (1.12) and (1.13). The group velocity has an opposite direction comparing to the phase velocity. This features the backward wave [11].

1.1.2 Effective-Medium Theory of Negative-Refractive-Index Metamaterials

A practical periodic 2-*D* transmission-line based NRI metamaterial can be realized using an array of unit cells each as depicted in Fig. 1.3. A host transmission-line medium (e.g. microstrip) is periodically loaded using discrete series capacitors and shunt inductors [12]. When the unit cell dimension d is much smaller than a guided wavelength the array can be regarded as a homogeneous, effective medium, and as such can be described by effective constitutive parameters $\mu_N(\omega)$ and $\varepsilon_N(\omega)$. The material parameters are determined through a rigorous periodic analysis to be of the form [14]:

$$\varepsilon_N(\omega) = \varepsilon_P - \frac{g}{\omega^2 L_0 d} \qquad (1.14)$$

$$\mu_N(\omega) = \mu_P - \frac{\frac{1}{g}}{\omega^2 C_0 d} \qquad (1.15)$$

Here ε_P and μ_P are positive constants describing the host transmission line medium and it is clear that this particular arrangement of the inclusions L_0 and C_0 provides the desired negative contribution that diminishes with frequency ω. The geometrical factor g relates the characteristic impedance of the transmission line network to the wave impedance of the effective medium. When the parameters are simultaneously negative these structures exhibit a negative effective refractive index [15].

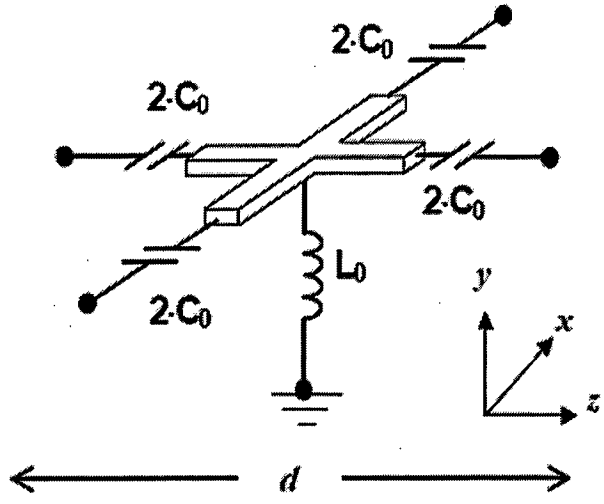

Figure1.3: Unit cell for the 2-D TL-based NRI metamaterial

During the work modified split ring resonator structure metamaterial was used. In the next section some of the metamaterial structures are briefly discussed.

1.1.3 Different Structures of Metamaterials

Left Handed Metamaterials have a lot of applications in Antennas so we will discuss different structures of it. We will discuss three types of Left Handed materials, Symmetric ring structure, Ω-like resonator structure and *S* shaped resonator structure.

1.1.3.1 Symmetric Ring Structure

Figure 1.4(a) and (b) show the configuration of split-ring resonator which was initially used at infrared frequencies [16] and which has been adapted to microwave frequencies. Compared with the SRRs/rods configurations in [17] two rings of this particular structure now have the same size and are symmetric with each other. The rod is placed on the opposite side of the substrate. Figure 7(c) shows a physically realized 1-*D* slab consisting of x × y unit cells. All the PC boards are pasted on a frame with a lot of slots which is made of organic plastic [18].

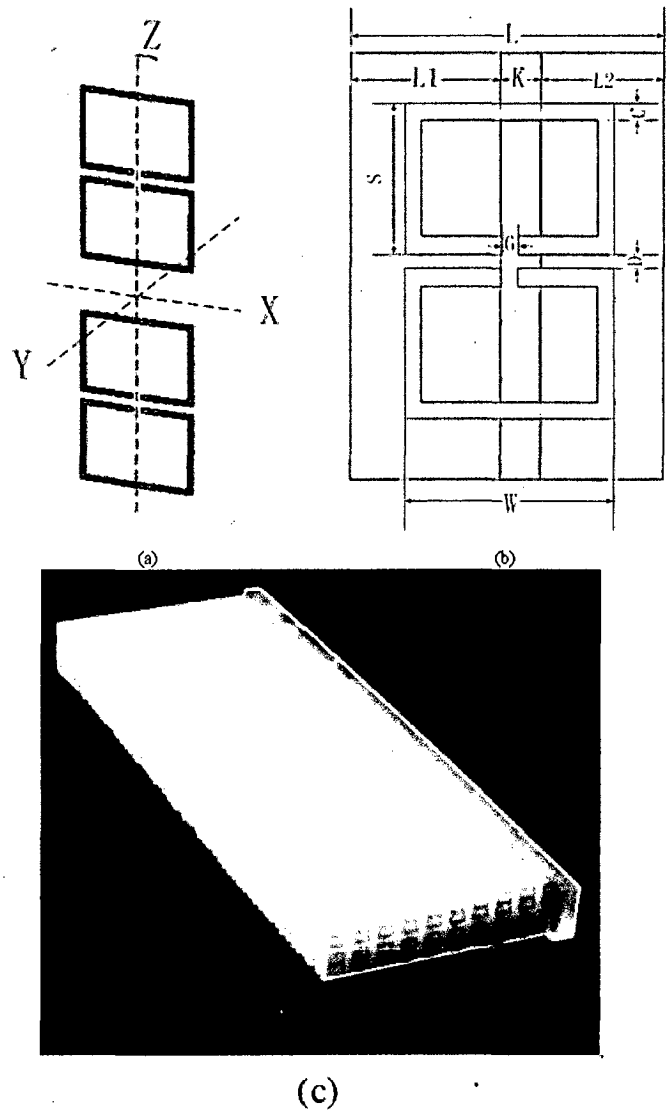

Figure 1.4: Dimensions of the symmetric ring structure and the photograph of a slab

1.1.3.2 Ω-like Resonator Structure

In this section we introduce another configuration of Left Handed Material which is fabricated by Ω-like metallic patterns and circuit board substrates. Our realization of Ω media is based on stacked Ω-like metallic patterns and repeated periodically. Fig 1.5 shows the dimensions of the basic unit cells and the photograph of the finished anisotropic metamaterial in which three Ω's are stacked in series to form a basic unit. Two such units are placed oppositely and closely in order to increase the coupling and avoid chiral effects. Figure 1.5 shows the basic unit cells of the Ω-like

structure with dimensions designated as *a*, *b*, *c*, *R*1 and *R*2. Three Ω's are connected in series to form the basic unit and a number of such units are placed side by side. The Ω's are printed on both sides of a substrate. Placing many pieces of this type of PC board side by forms a rectangular metamaterial [18].

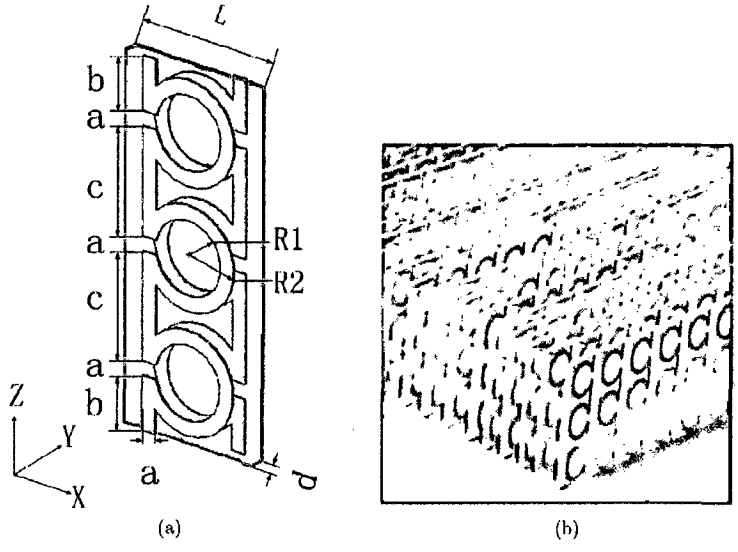

Figure 1.5Dimensions and realization of Omega media.

1.1.3.3 S-Shaped SRR Structure

In this section we study a metamaterial structure which is composed of a series of *S*-shaped resonators [19] connected with each other. Such a metamaterial has been shown to exhibit low losses and a left-handed behavior over a large frequency band. A sample of the metamaterial is shown in Fig. 1.6.

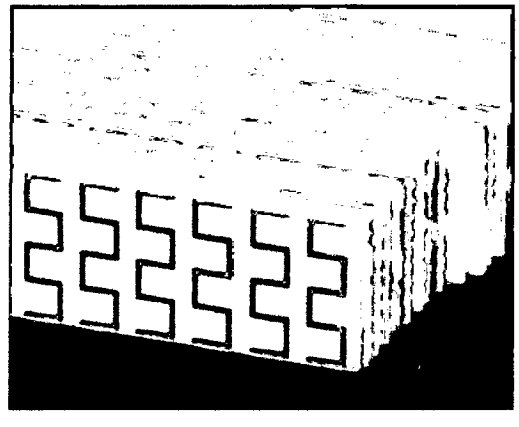

Figure 1.6Metamaterial composed of '*S*'-shaped SRR.

1.2 Introduction to Patch Antennas

The idea of microstrip antenna dates back about half a century to the work in USA by Deschamps [20] and independently by Gutton and Baissinot in France. Further, the work was carried out by Munson [21] on the development of microstrip antenna for use as low-profile flush-mounted antennas on rockets and missiles. This work showed that microstrip antenna was a practical concept for use in many antenna system problems, and thereby gave birth to a new antenna industry. Over all these years, microstrip antennas have gained enormous utility in the field of wireless communication due to their versatility.

These are low weight, low volume and low fabrication cost antennas and hence can be manufactured in large amounts. These low profile planar configurations which are capable of dual and triple frequency operation and support both linear and circular polarization can be easily made conformal to host surface. Further, these can be integrated with MIC and are mechanically robust when mounted on rigid surfaces. Due to these advantages, they have found applications in a wide variety of wireless infrastructures. These are used for satellite communication as telemetry and communication antennas on missiles. Also, they are compatible with handheld wireless devices such as cellular phones, pagers etc. as embedded antennas [22]. These also have been found to be well suited for modern WLAN applications.

However, these antennas have several disadvantages as compared to their conventional counterparts. A simple patch antenna has a narrow bandwidth, low power handling capability, low efficiency, poor polarization purity, poor scan performance and spurious feed radiation. Ever since the advent of these antennas, much of the work has been done to overcome these disadvantages to make these patch antennas suitable for wireless applications, especially to increase the bandwidth of the antenna. There are a number of such methods available today which involve certain modifications in a simple patch to vary its properties according to a particular application. A lot of research has been done on these bandwidth enhancement techniques in past decades. The need of these techniques arises since the bandwidth requirements of present day wireless applications is much higher than the bandwidth of a simple patch antenna (1-2%). The required

operating bandwidths for antennas are 7.6% for a global system for mobile communication (GSM; 890-960 MHz), 9.5% for a digital communication system (DCS; 1710-1880 MHz), 7.5% for a personal communication system (PCS; 1850-1990 MHz), and 12.2% for a universal mobile telecommunication system (UMTS; 1920-2170 MHz). A detailed account of such studies on broadband microstrip antennas has been summarized in [23]. Structure of basic microstrip antenna has been given in Chapter 2.

1.3 Motivation and Scope

Remote sensing is very potential application field of RF and Microwaves. Its area of application extends from daily life navigation to modern warfare. Remote sensing is the acquisition of information about an object or phenomenon, without making physical contact with the object. In modern usage, the term generally refers to the use of aerial sensor technologies to detect and classify objects on Earth (both on the surface, and in the atmosphere and oceans) by means of propagated signals (e.g. electromagnetic radiation emitted from aircraft or satellites).The antennas used for this purpose have rigid space constraint with enhanced performance. The modern antennas used in remote sensing satellites are converging towards planar structure compared to the earlier bulky designs. The aim of the dissertation is to realize an L-Band antenna operating at 1.28 GHz with reduced size compared to its conventional counterpart. The above specification is according to the ongoing project of ISRO.

The exact problem statement is given in the next section and the design studies and results have been presented in the following chapters of the thesis.

1.4 Problem Statement

a) Literature survey for metamaterial application in planar antennas.
b) Planar antenna design at L-band (1.28 GHz).
c) Requirements with metamaterial
    i. Size reduction of about 40%
    ii. Feeding : Coplanar or any other kind except co-axial

1.5 Organization of the Dissertation

There are five chapters compiled in this dissertation including the present chapter.

- ***Chapter one*** gives a brief theory of metamaterials and microstrip patch antenna. All the basic concepts are discussed like properties of metamaterial and its different structures.
- ***Chapter two*** presents the related literature survey of applications of metamaterial to microstrip patch antennas for various performance enhancement and size reduction.
- ***Chapter three*** describes the Design methodology, analysis procedure adopted for the design of microstrip patch antenna and proposed Metamaterials resonator.
- ***Chapter four*** deals with the design studies and simulation results of different antennas proposed for this dissertation. The fabrication and measurement results of all the resonators have been given and discussed.
- ***Chapter five*** concludes the thesis with the concluding remarks and outline direction for future scope.

Chapter 2
Literature Survey

The most basic form of microstrip antenna, also called patch antenna consists of radiating patch on one side of the substrate which has ground plane on the other side Fig. 2.1. The patch is generally made of metal like copper, gold etc. which can take any possible shape. The radiating patch and the feed lines are generally photo-etched or dry-etched on the dielectric substrate. Common shapes like rectangular, triangular, circular, elliptical or practically any shape are often used to simplify the analysis and performance prediction.

Primarily, microstrip patch antennas radiate due to the fringing fields between the patch edge and the ground plane. For good antenna performance, a thick dielectric substrate having a low dielectric constant is desirable since this provides better efficiency, larger bandwidth and better radiation. However, such a configuration leads to a larger antenna size. In order to design a compact microstrip patch antenna, higher dielectric constants must be used which are less efficient and result in narrower bandwidth. Hence a compromise must be reached between antenna dimensions and antenna performance.

Microstrip patch antennas can be fed in a number of ways. These are basically classified into two categories- contacting and non-contacting. Commonly used methods are microstrip feed and co-axial feed (both are contacting methods), aperture-coupled feed and proximity-coupled feed (both are non-contacting methods).

One of the simplest methods of analysis of a microstrip antenna is transmission line method. In Fig. 2.1, most of the electric field lines reside in the substrate and parts of some lines in air. Hence, TEM mode cannot be supported; quasi-TEM is the dominant mode. An effective dielectric constant ϵ_{eff} must be obtained in order to account for the fringing and the wave propagation in the line. The value of ϵ_{eff} is slightly less than ϵ_r because the fringing fields around the periphery of the patch are

not confined in the dielectric substrate but are also spread in the air as shown in Fig. 2.1.

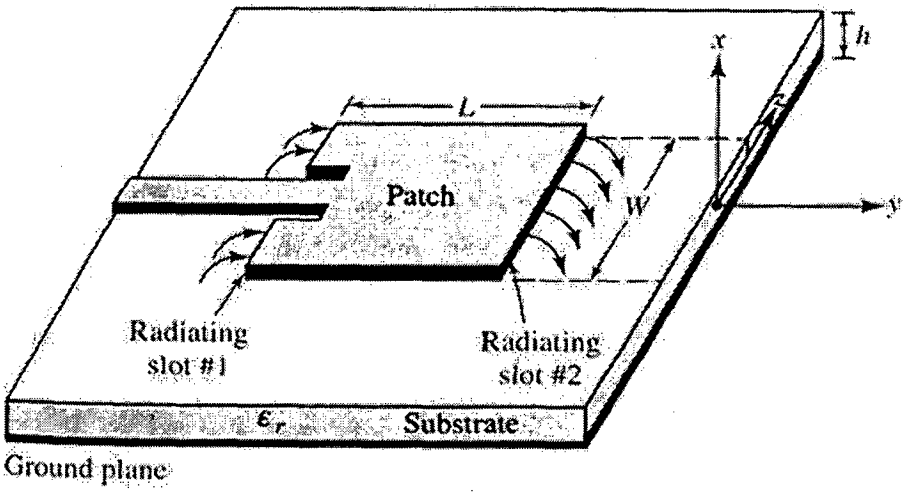

Figure 2.1: Microstrip Patch Antenna structure [22]

2.1 Application of Metamaterials to Microstrip Patch Antennas

2.1.1 Reduction of mutual coupling

Mutual coupling between elements in an array comes from two ways. The first one is from free space which is present in all types of arrays. The second one arises from surface waves which becomes very important in case of patch antenna array. In this type of antennas surface waves are strongly excited when patch antennas are operated in fundamental mode (*TM*10 for rectangular patch antenna). In this mode the field distribution inevitably excites the first propagation mode of surface wave in E plane. Moreover the use of thick or high permittivity surface enhances this excitation. Periodic structures like EBG (Electronic band gap) have the ability of suppressing the surface waves. Consequently their use in reduction of surface wave is straight forward. In case of array antennas we also can place the subsequent elements very close to each other since its surface waves are already suppressed by EBG structures making the array very compact [4]. A typical application of mutual

coupling reduction is reported in [24]. In this paper the authors used EBG substrate to suppress the surface wave so as to reduce the mutual coupling by keeping the elements nearer than λo(free space wavelength). Comparison of mutual coupling in presence of EBG ground plane in absence of EBG ground plane has also been carried out by the authors. Effects on mutual coupling by varying the number of EBG elements and by varying the distance between the patch units was also studied.

2.1.2 Enhancement of Directivity

Periodic metallic structure has the ability to simulate various homogeneous materials whose specific properties eventually do not exist for natural materials. It has been shown that the structures composed of periodic mesh of metallic thin wires, when its characteristics dimensions are small in comparison to the wavelength behaves as a homogeneous materials with low plasma frequency. It means that the dispersion relation of the propagation modes in this structure shaped like plasmas of electron gas. This opened the fields of composite materials or metamaterials for microwave or optical application. Theoretical and experimental work has shown that such arrays of continuous wires are characterized by a plasma frequency. Both approximate analytical theory and rigorous homogenization theory show that equivalent behaviour has a behaviour governed by a plasma frequency in microwave domain.

The first consequence of this microwave plasma frequency is that the equivalent permittivity is negative when the operating frequency is below the plasma frequency. The other extraordinary property is that the permittivity is positive and less than one. That is to say the optical index is less than one or very close to zero. This property of the material helps in enhancement of directivity in the following way. Let us consider a point source inside a slab of near zero index material surrounded by homogeneous isotropic materials as shown in the Fig. 2.2.

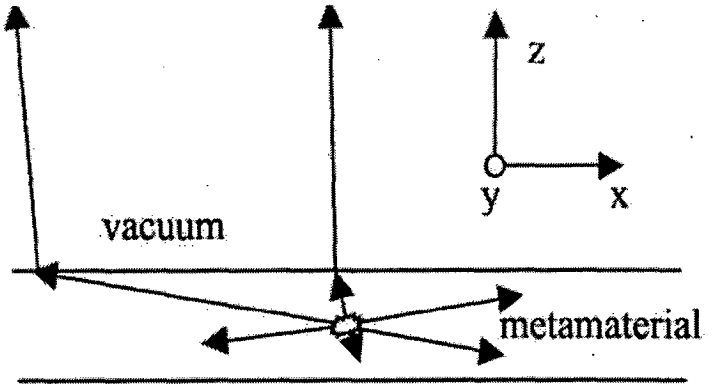

Figure 2.2: Point source inside a slab of near Zero index material

We consider an incident ray on an interface with grazing incidence that comes from a source inside the slab of Metamaterials. The Snell-Decarte's laws imply that with non zero index the ray in the media above the slab will be refracted in a direction very close to the normal (lower is the optical index, closer is the direction towards the normal).Then almost all the rays will be in the same direction around the normal. Hence almost all the rays will be directed perpendicular to the surface there by increasing its directivity [25].

Application of the above mentioned theory can be seen in [26]. In this paper the authors have designed a horn antenna filled with metamaterial structures. In this horn aperture, three layers of fine metal grids and foams were fixed which acts as a metamaterial. In case of ordinary horn antenna E field distribution spreads gradually and there is significant decrease of E field at several λ away from the horn. On the contrary when horn with metamaterial is used there is enhanced E field at several λ away from the horn as expected.

2.1.3 Enhancement of return loss and radiation pattern of a low profile antenna

EBG embedded ground plane has an interesting property of variable reflection phase. For instance if a plane wave falls on an EBG ground plane normally then the phase of the reflected wave (known as reflection phase) varies from π to $-\pi$ depending on frequency. The same reflection phase for PEC and PMC ground plane are π and 0 respectively. So if we use a low profile antenna placed very near to ground plane, then reflections from the ground plane distorts the return loss as well

as radiation pattern in case of PEC or PMC materials. On the contrary the usage of EBG ground plane, by properly selecting the frequency one can overcome this distortion up to a great extent due to its variable reflection phase [27].

In the above mentioned paper the authors have simulated a low profile dipole antenna based on FDTD method with PEC, PMC and EBG ground planes. Here they have found with the usage of EBG ground plane the return loss improved a lot compared to their PEC and PMC counterparts.

It was already discussed that EBG ground plane can also be used to suppress the surface waves. In most of the cases the band gap does for surface wave suppression does not coincide with that of the frequency band in which EBG has a good phase reflection characteristics. In this paper authors have devised a FDTD based model which helps us to choose the frequency band for an EBG which satisfies both the criterion mentioned above.

2.1.4 Reduction of antenna size

Due to the unique nature of the Zeroth order mode the size of the resonator does not depend on its physical size but only on the amount of reactance provided by its unit cell. A potential advantage of the Zeroth order antenna is constant magnitude field distribution. The correspondingly perfectly even repartition of energy along the structures leads to a small ohmic losses than in other small antennas where current concentration near discontinuity produces high losses. Consequently high efficiency factor K can be achieved in the Zeroth order antenna which can mitigate to some extent reduction in gain subsequent to size reduction. Another Zeroth order effect helping to achieve optimal gain for a given physical size of the antenna is the fact that the effective aperture is increased and becomes larger than that of a typical antenna resonating in its first mode [4]. As the objective of my project was size reduction of L-Band antenna so few papers in which there was size reduction using metamaterial were studied and discussed below.

Realization of a small resonant antenna design using metamaterial can be seen in [28].Here the authors have used CRLH transmission line to design an electrically

small antenna. The physical size and operating frequency of the antenna depend on the unit cell size and equivalent transmission line parameters. The length, width and height of the antenna is 1/19λ0, 1/23λ0 and 1/83λ0 Corresponding to n=-1, n=-2 and n=-3. The resonance frequencies obtained was $f1$ = 1.06 GHz, $f2$ = 1.06 GHz and $f3$ = 1.06 GHz. At the above mentioned frequencies antenna has fair amount of return loss of -10.5 dB, -4.9 dB and -4.2 dB respectively.

Another technique of antenna size reduction using spiral resonator is reported in [29].Here the authors have used spiral loop which produces magnetic property in natural dielectrics. The spiral loops itself acts as an inductor. Also there is distributed capacitance effect in between the turns of the spiral. This spiral inductance and spiral capacitance causes the resonant behaviour. In this metamaterial substrate the permeability is enhanced for Y directed magnetic fields and permittivity enhancement will occur for X or Z directed electric fields. This combination permeability or permittivity is exactly same as that needed for support of modes in microstrip patch antenna. Moreover the effective permeability of this substrate depends on the frequency and therefore they yields different miniaturization factor at different frequency. For conventional ground plane if the physical size is reduced by a factor of 2 then the increase of frequency is also by a factor of 2. In contrast for this substrate 50% decrease in physical size will make a change of frequency by 20%.

[30]This paper proposes a small patch antenna on metamaterial substrate. The antenna was designed for X-band application with a specific cutoff frequency at 11.28 GHz. The metamaterial substrate has a potential to reduce the circuit size of the antenna as well as maintain the amplitude of the return loss at the specific resonant frequency. The most attractive feature of the substrate is the ability of enhancing the bandwidth of a patch antenna. The newly invented metamaterial antenna contributes the best return loss of more than -20 dB and 300 MHz bandwidth wider than the conventional patch antenna. The size of the metamaterial antenna has been reduced by a factor of 2. The invented metamaterial was constructed from a combination of two materials which are the Flame Retardant 4 (FR-4) and copper metal in a symmetrical-ring. The S-parameters from the

computer simulation technology (CST) are proven the negative permittivity. This metamaterial antenna has high potential in the future telecommunication industries in enhancing the performance of the technology for consumers. A metamaterial substrate has been successfully designed and proven to be negative permittivity along the range of frequencies. That new material was obtained due to the unique structure. The Implementation of the metamaterial as the substrate in a patch antenna could reduce the overall circuit size to be half of the conventional design. The return loss magnitude of the antenna at resonant frequency is still maintained to be more than -20 dB. The advantage of the metamaterial antenna is the ability to produce 300 MHz bandwidth wider than to the conventional antenna.

[31] This paper recommends a compact circular patch antenna on metamaterial substrate for C-band applications. The antenna is designed for some improvement in the performance of directivity gain; return loss and size of circuit area. The size of the new metamaterial antenna has been reduced by a factor of 2.4 and the directivity gain was increasing from4.17 dBi in conventional design on Flame Retardant 4 (FR-4) to 5.66 dBi in the new approach. A better return loss was obtained from the metamaterial antenna which is -24.2 dB compared to -22.08 from the conventional antenna. By analyzing the radiation pattern, the metamaterial antenna has a sharp focus to the targeted direction. The compact antenna is expected to improve the cost of production due to the size reduction in the overall circuit area especially in a mess production. This investigation shows that the split ring structure able to produce a metamaterial substrate. It has been successfully proven by the negative permittivity in the range of 4.6GHz to 4.9GHz. Applying the metamaterial in designing patch antenna is able to reduce size of the circuit area more than 50% of the overall dimensions. It is also able to improve the return loss from -22 dB to -24 dB as well as 1.5 dBi directivity gain higher than the antenna on FR-4.

[32] In this paper a rectangular miniaturized patch antenna loaded by new metamaterial unit cells, which operate as mu-negative medium, is proposed. The unit cell is made of a spiral and three wires printed on a dielectric that resonance is 3 GHz. The results of return loss and radiation pattern at the sub

wavelength resonances on patch antenna are reported. The patch dimensions are 8×12 mm that resonance in 5.05 GHz. But, the proposed antenna that loaded by 6 unit cells resonance at 3.19 and 3.76 GHz, which correspond to about 40% and 30% size reduction and by 10 unit cells resonance at 3.89 GHz, which corresponds to 25% size reduction that in these frequencies the radiation pattern of antenna are increased. A miniaturized rectangular metamaterial patch antenna loaded with MNG material presented. The MNG metamaterial is made combination of spirals and 3 wires that are printed on both sides of a dielectric. The permeability of unit cell is negative at the frequency of 3 GHz. Antenna performance measured and reported in two form namely with and without metamaterial load. The resonance frequency of antenna without metamaterial is 5.05 GHz. But, it was shown that it is possible to reduce antenna size about 40% and 30% with 6 numbers of unit cells. In order to understand the performance of proposed antenna, the radiation pattern in new resonance frequencies described. At lower resonance frequency the radiation pattern increased about 4.5 dB and in middle resonance frequency increased about 3 dB. Also, the antenna with 10 number unit cells reported.

[33] In this paper they presented characteristics of microstrip patch antennas on metamaterial substrates loaded with complementary split-ring resonators (CSRRs). The proposed antenna utilizes CSRRs in the ground plane altering the effective medium parameters of the substrate. To characterize the performance of the CSRR loaded microstrip antenna, the metamaterial substrate has been modeled as an effective medium with extracted constitutive parameters. Simulation results were verified by experimental results. The experimental results confirm that the CSRR loaded patch antenna achieves size reduction as well as bandwidth improvement. A compact microstrip antenna with an improved bandwidth using a metamaterial substrate based on complimentary split ring resonators has been presented. For the characterization of the microstrip antennas on metamaterial substrates, the effective medium approach was employed. The new design help achieve the reduction of the antenna size and the improvement of the bandwidth for microstrip patch antennas. Interesting Zero th order resonances have been observed in the proposed antenna, which could be useful in designing multiband antennas.

Chapter 3
Design Methodology

This chapter consists of the design methodology used for this project which includes the descriptions on the selected metamaterial structure, the design calculation of the metamaterial structure and the patch antenna.

The methodology adopted in this design includes the numerical approach in which the basic parameters are first being calculated using the corresponding formula. The designed structure is then being simulated using a simulation tool and the simulation results are being compared to the calculation and theoretical result. The methodology described here is illustrated in Fig. 3.1.

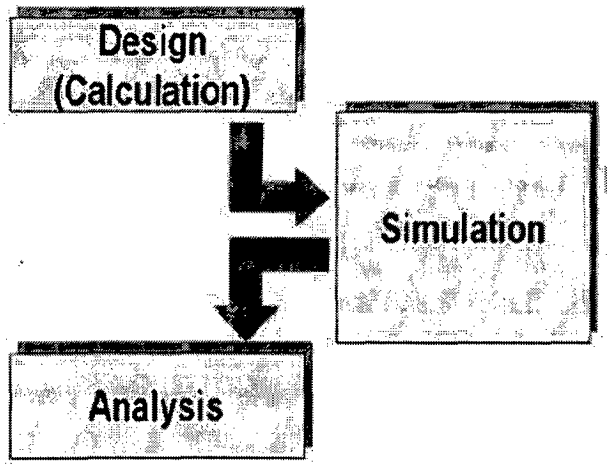

Figure 3.1: Design methodology steps

Metamaterial or LHM is a composite, whose properties are not determined by the fundamental physical properties of their constituents but by the shape and distribution of specific patterns included in them. The structure can be designed in many way, however the fundamental concept and theory of the structure and its properties is very important since it will determine the ability to produce the LHM behavior in the required frequency band. The design starts with the metamaterial structure which is conventionally composed of split ring resonator (SRR). The

periodic SRR structure provides negative effective permeability. The SRR is designed to meet the limitations that the experimental setup required due to the use of the waveguide. It was printed on a FR4 substrate with dielectric constant of ϵr = 4.4 and loss tangent tan δ = 0.0024. The thickness of the substrate is 1.524 mm.

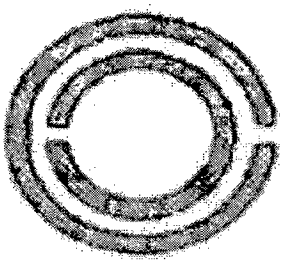

Figure 3.2: Split Ring Resonator structure

The dimensions of the substrate and the SRR are adjusted accordingly in order to get the desired working frequency range. The SRR consists of two metallic micro strip rings with a slit (or gap) which may be different in shape such as circular or square rings. There are several parameters that need to be tuned including width and height of the micro strips, distance between the rings, size of the gap, material properties of the rings, substrate and surrounding medium in order to get the desired negative permeability property at certain frequency range. The dimensions of the unit cell and the spacing of unit cells in an array determine the desired effective negative index of permeability in case of SRR. The SRR structure is shown in Fig. 3.2. During my project modified SRR was used.

The simulation starts with the calculated values of different design parameters for a specific dielectric material (here it is FR4). The calculated values are best initial guess of all the parameters for the specific goal i.e. resonant frequency and band width. The design is made in the CAD tool integrated with the CST MWS. The simulation parameters like frequency span over with response to be calculated, boundary conditions, excitation mode and impedance matching were done. Defining port is a critical parameter while using CST MWS. Proper dimension is to be set for proper port impedance and mode of excitation. Proper meshing of different regions depending on the complexity nature of the design has to be done.

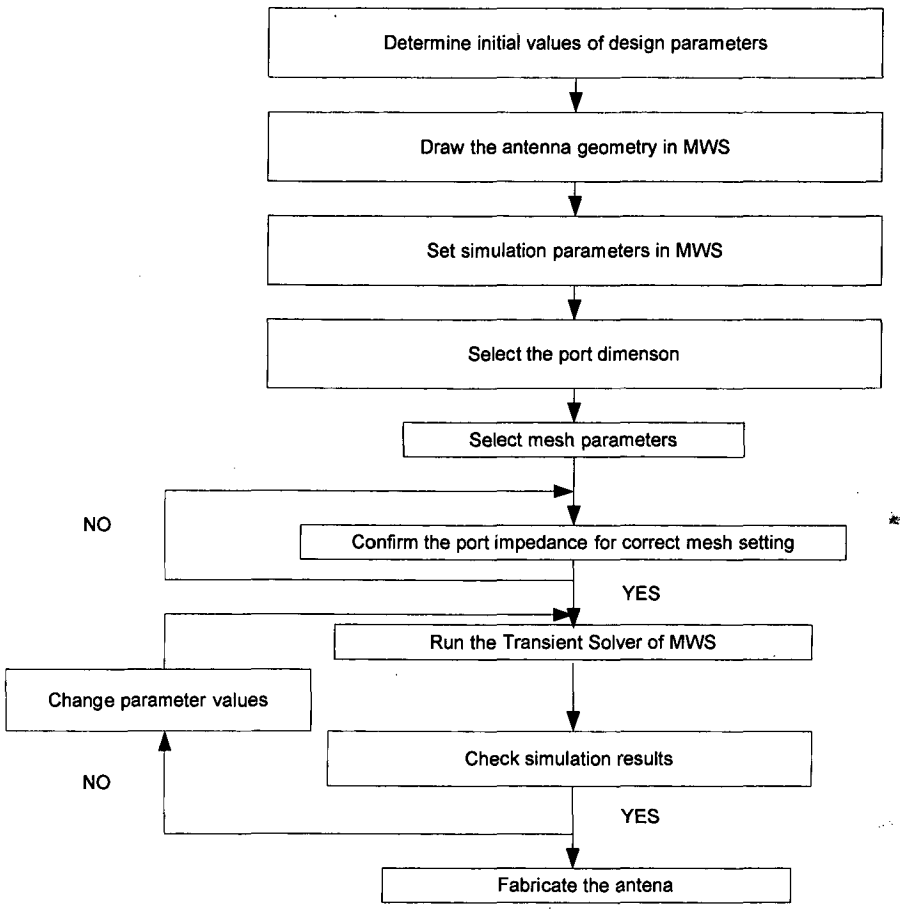

If the design port mode is achieved, then start simulation otherwise correct the mesh settings. Generally transient solver is preferred for antenna simulation, because it solves for the whole frequency span at a single run. After simulation, results are to be checked. If the results are not satisfactory, the corrections have to be made to the design and values of design parameters is to be done. The processes are repeated till the desired results are met. After that the design is fabricated and tested for its return loss and radiation pattern.

Chapter 4
Design, Simulation and Measurement results

4.1 Microstrip Patch Antenna for L-band (1.28 GHz) applications

In this section design studies, parametric analysis, simulation results along with measurement results for a simple planer rectangular microstrip patch antenna with insert feeding technique is presented. All the designs are fabricated in LPKF S100 machine with dry metal etching.

4.1.1 Antenna Geometry and Parametric analysis

The antenna configuration of the rectangular resonator structure is shown in Fig. 4.1 with the dimensional notations. The gray color portion is the metallic part. The metallic resonator structure is on a commercially available low cost FR4 dielectric substrate with $\varepsilon_r = 4.4$, thickness of substrate is 1.524 mm with loss tangent 0.0024. The physical dimension of the rectangular patch is calculated according to the formula in C.A. Balanis. The calculated length (pl) to operate at 1.28 GHz is 54.5 mm. For simplicity the width (pw) and length (pl) were taken equal. A feed line of characteristic impedance as 50 Ω is adopted to feed the patch with insert mechanism. The width of the feed line (fd) was 2.8 mm to achieve 50 Ω. A square substrate of dimension 70 mm x 70 mm is used.

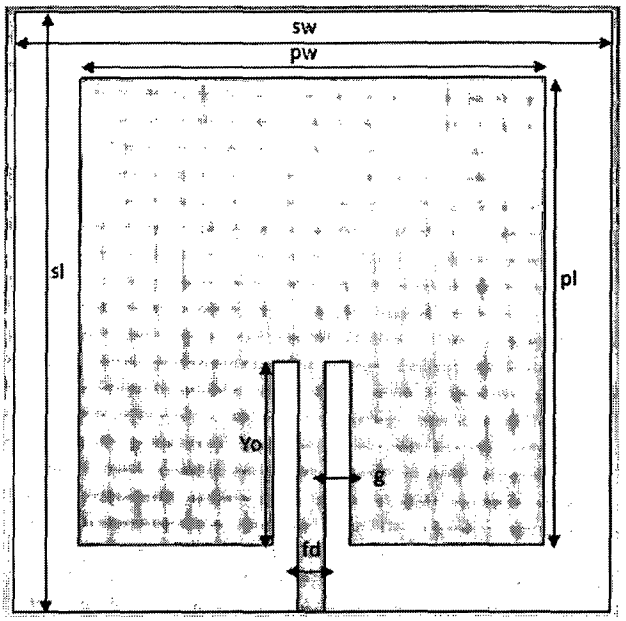

Figure 4.1 Rectangular Microstrip Patch antenna with Insert Feed

Typical simulated return loss is shown in Fig. 4.2 and Fig. 4.3 shows the parametric variation of patch length. From the figure it can be observed that the inverse relation between resonant frequency and patch length is well verified.

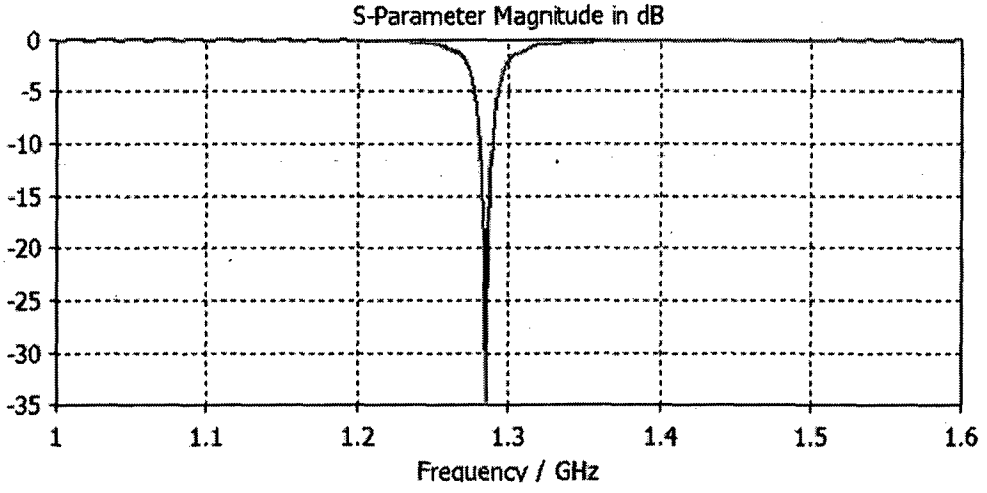

Figure 4.2 Simulated Return Loss

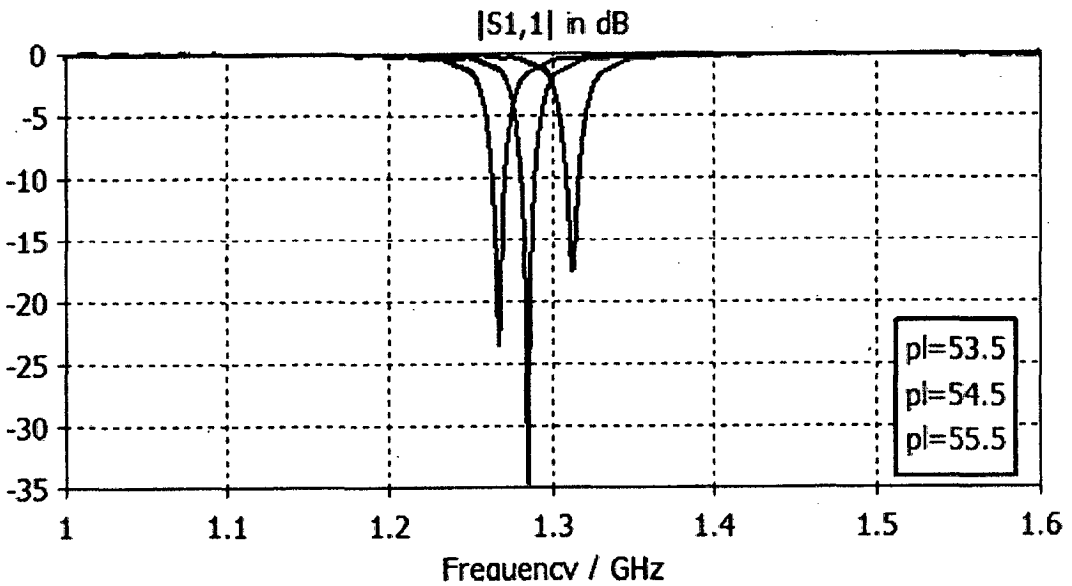

Figure 4.3 Variation of resonant frequency with patch length (pl)

The Fig. 4.4 shows the parametric analysis of patch width. One can see that the change in the patch width around the tuned condition, fairly affects the resonance frequency except the level of impedance matching, which is according to the theory of patch antenna.

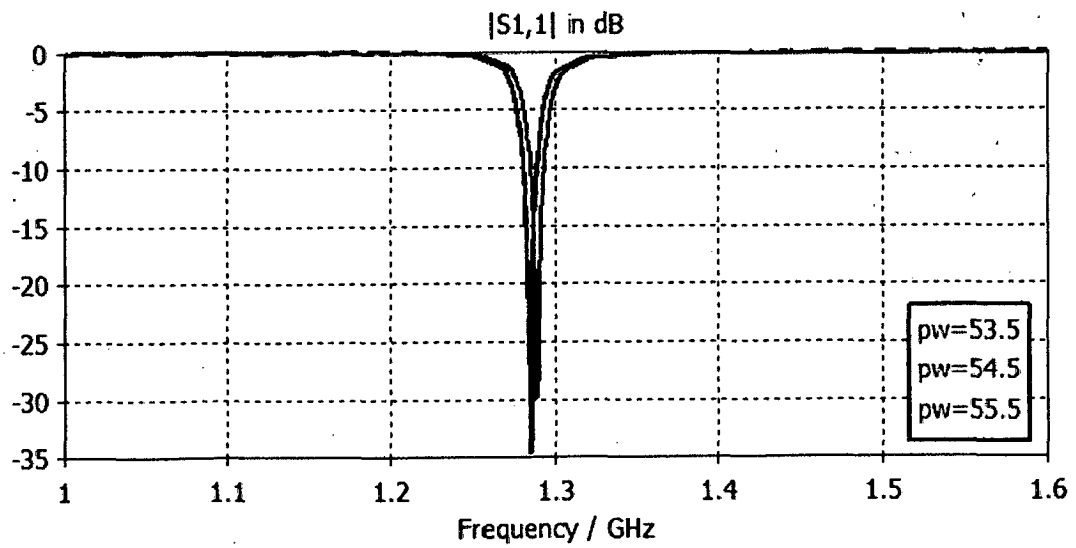

Figure 4.4 Variation of resonant frequency with patch width (pw)

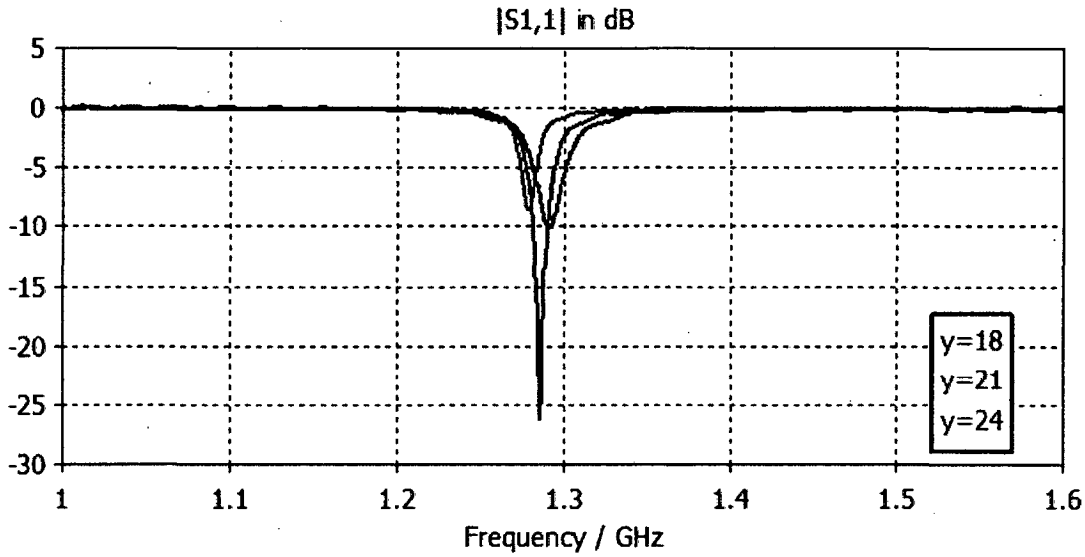

Figure 4.5 Variation of resonant frequency with insert length (y)

Above Fig.4.5 shows the variation of impedance matching with variation of insert length. It can be seen in the figure that if we increase or decrease the insert length from y=21 we get reflection losses due to impedance mismatch and return loss less than 10 db.

4.1.2 Fabrication and Measurement Result

The rectangular patch antenna after optimization and analysis was fabricated and tested in the laboratory. Fig. 4.6 shows the fabricated antenna and measured return loss being tested on HP network analyzer (HP 8720B). The radiation performance has been measured in the anechoic chamber keeping the fabricated prototype at receiver end. About 15dBm power was given to the transmitter antenna from the RF power generator, and the distance between the transmitter and the receiver was kept at 1.5 meter.

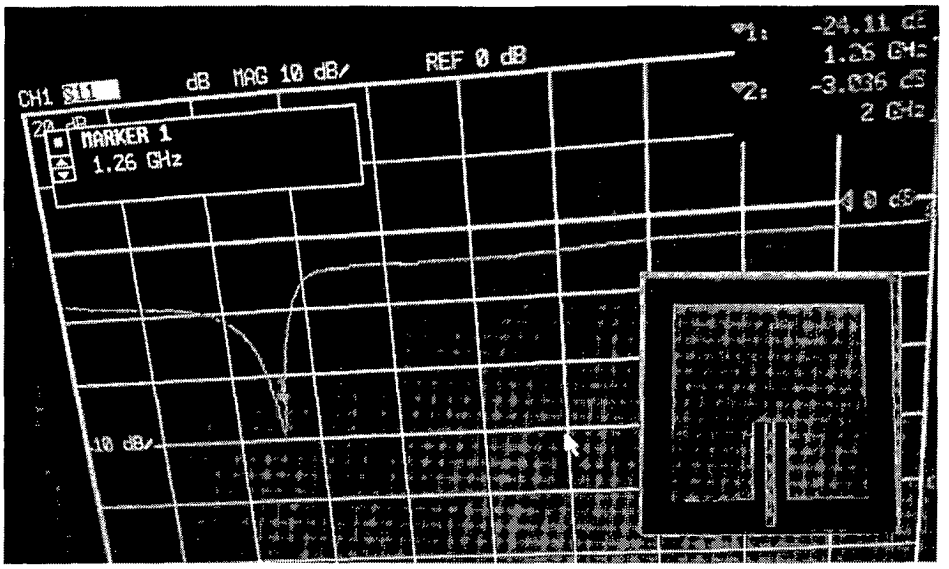

Figure 4.6 Fabricated antenna and measured return loss

The fabricated antenna was tested for its far-field radiation properties. Measurement were done for pattern in its both the planes (*E*-plane and *H*-plane power pattern). Fig.4.7 shows the simulated and measured radiation patterns of the antenna in both the *E*-plane and the *H*-plane.

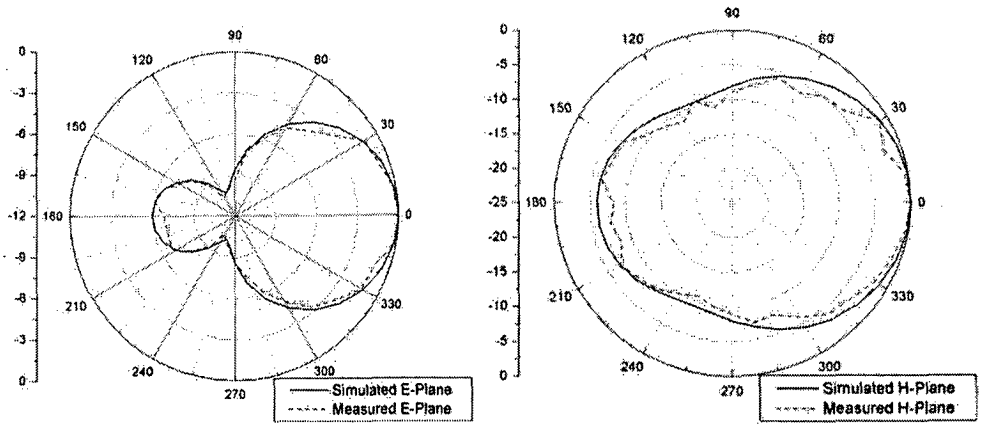

Figure 4.7 Simulated and Measured Radiation pattern

These plots confirm the broadside directive radiation properties of the antenna. The simulated and measured radiation patterns are in close agreement except some ripples at the measured results. The measured radiation pattern in both *E*-plane and *H*-plane are somewhat distorted compared to that of simulated patterns. This may

be due to the fact that low power levels are received by the antenna. Possible reasons for these disagreements between simulated and measured results may due to the possible presence of interference and noise. The achieved impedance bandwidth (measured at -10 dB refection coefficient) is around 100MHz. The simulated gain was about 4.7 dB.

4.2 Design 1: Modified Split Ring Resonator for L-band (1.28 GHz) applications

During the dissertation a novel modified SRR is proposed for L-band (1.28 GHz) applications is proposed. An H-field coupling feed method is adopted with reduced ground plane. A notable size reduction of 81% in size is achieved with reasonable simulated gain.

4.2.1 Antenna Geometry and Parametric analysis

The antenna configuration of the proposed resonator structure is shown in Fig. 4.8 with the dimensional notations. The gray color portion is the metallic part. The metallic resonator structure is on a commercially available low cost FR4 dielectric substrate with $\varepsilon_r = 4.4$, thickness of substrate is 1.524 mm with loss tangent 0.0024. A feed line of characteristic impedance as 50 Ω is adopted to feed the resonator. The width of the feed line (fd) was 2.8 mm to achieve 50 Ω. A square substrate of dimension 30 mm x 30 mm is used.

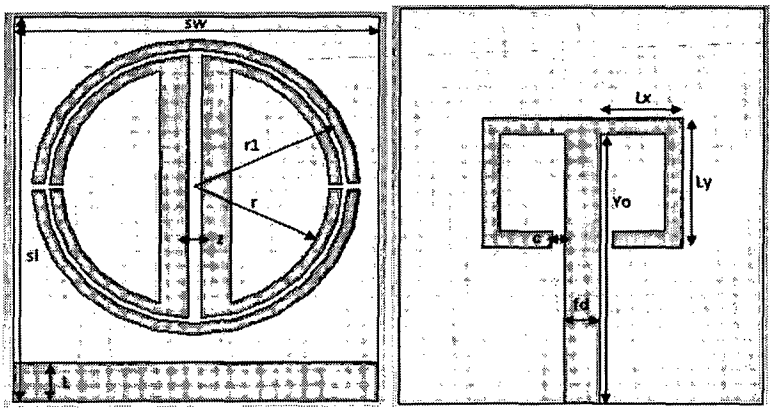

(a) (b)

Figure 4.8 (a) Top View (b) Back View of the resonator

Simulated return loss for above design is shown below. It can be observed that it is much less than -10 db as required.

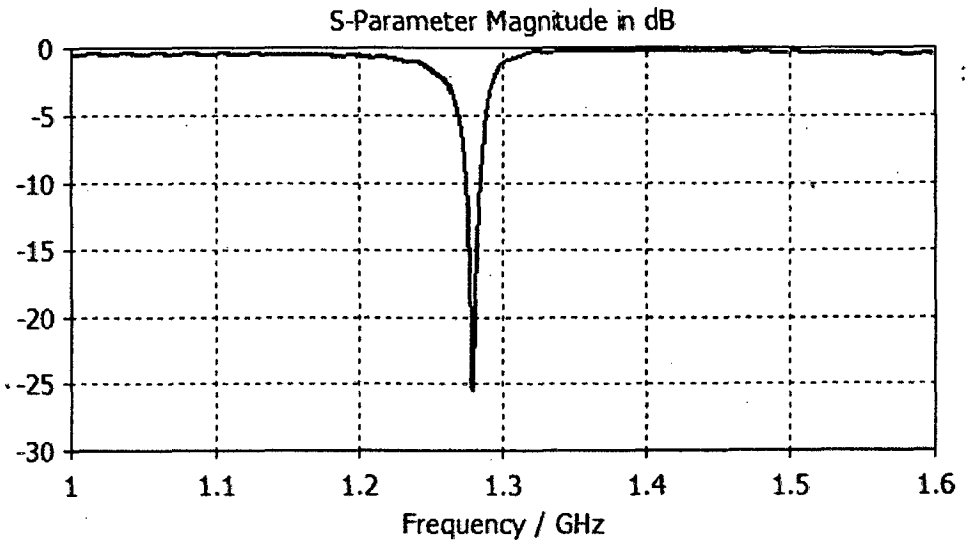

Figure 4.9 Simulated return loss

Surface current distribution is shown below in the diagram. Direction of current in the given design can be noted in the figure.

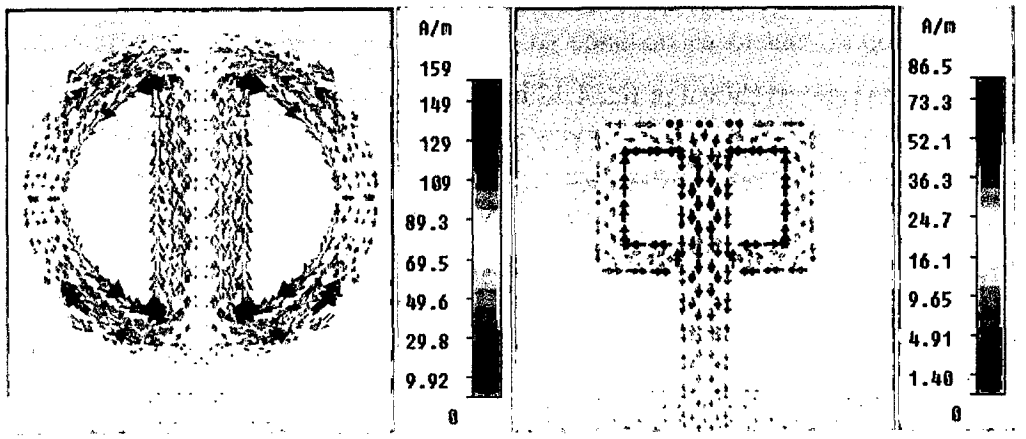

Figure 4.10 Surface current distributions at 1.28 GHz

The microstrip feeding network and the resonator are in opposite sides of the dielectric substrate. As seen from the figure, the gap (c) of 1mm in the feeding network causes discontinuity in the electrical path. The changing electric current results magnetic flux loops. These changing magnetic flux when pass through the loops of the SRR, induces an electric current Fig.4.11. The integrated inductance of transmission line and gap capacitance forms a resonator tank circuit operating at 1.28 GHz frequency.

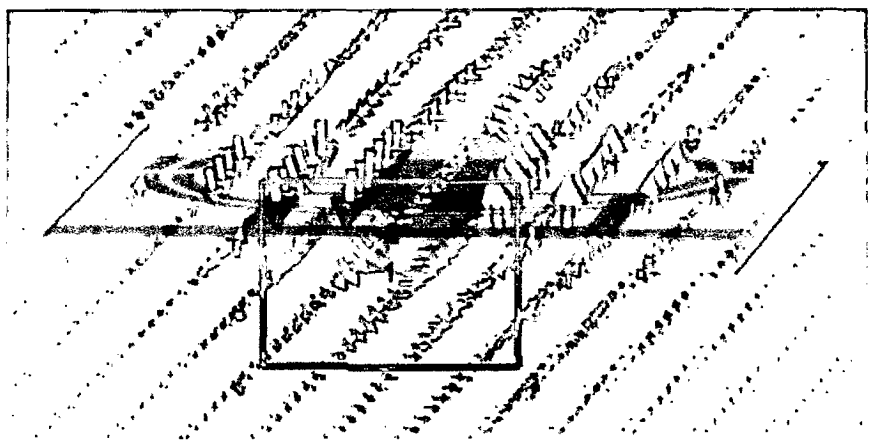

Figure 4.11 H-field distribution at 1.28 GHz

The resonance can be easily tuned with a more number of degree of freedom modifying the design variables like inner ring radius (r), outer ring radius (r1) and gaps in rings (g & g1). A detail parametric analysis is done to understand the design. As we increase the outer radius (r1), the capacitance should decrease as the distance between two rings is increasing. As we know that the resonant frequency is inversely proportional to capacitance so on increasing r1 the resonant frequency should shift to right as shown in fig. 4.12 below.

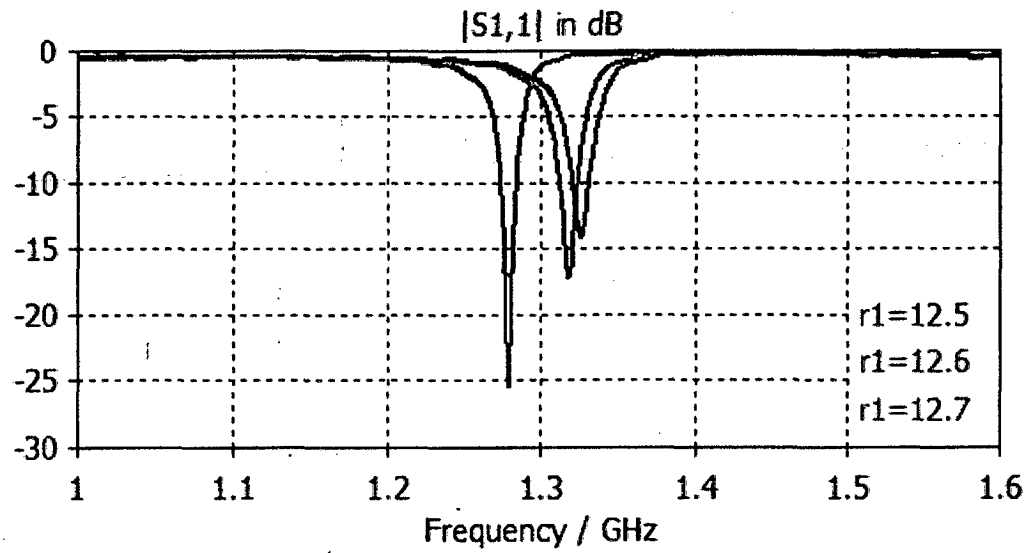

Figure 4.12 Variation of resonant frequency with outer ring radius (r1)

As we decrease the inner radius (r), the capacitance should decrease as the distance between two rings is increasing. As we know that the resonant frequency is inversely proportional to capacitance so on decreasing (r) the resonant frequency should shift to right as shown in fig. 4.13 below.

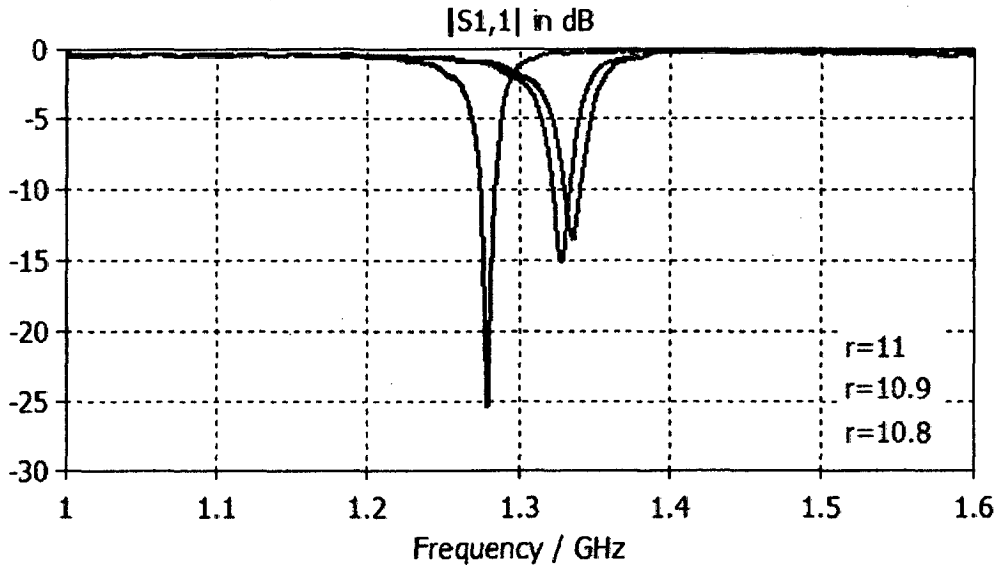

Figure 4.13 Variation of resonant frequency with inner ring radius (r)

As we increase the gap in between the inner ring (g) the capacitance decreases and there is right shift in resonant frequency as shown in the fig. 4.14 below.

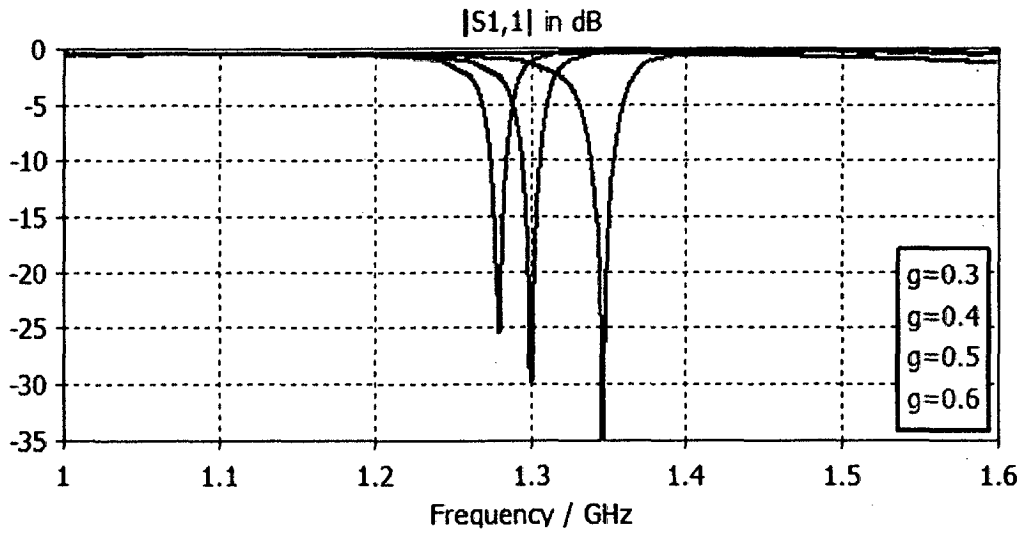

Figure 4.14 Variation of resonant frequency with inner ring gap (g)

Similarly as we increase the gaps in between the outer ring (g1) the capacitance decreases and there is right shift in resonant frequency as shown in the fig. 4.15 below.

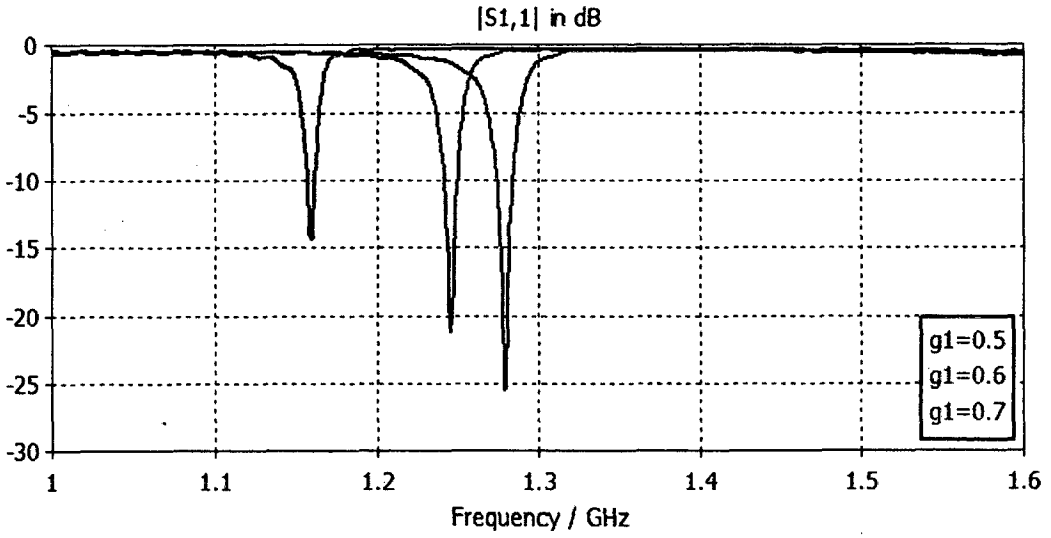

Figure 4.15 Variation of resonant frequency with outer ring gap (g1)

In this section we discussed the parameter sweep i.e. effect of varying various parameters of the given design on the resonant frequency of design. It has been shown that it shifts either right or left. In the next section we will discuss fabrication and measurement results.

4.2.2 Fabrication and Measurement Result

The proposed modified SRR after optimization and analysis was fabricated and tested in the laboratory. Fig. 4.16 shows the fabricated antenna and measured return loss being tested on HP network analyzer (HP 8720B). The radiation performance has been measured in the anechoic chamber keeping the fabricated prototype at receiver end. About 15dBm power was given to the transmitter antenna from the RF power generator, and the distance between the transmitter and the receiver was kept at 1.5 meter.

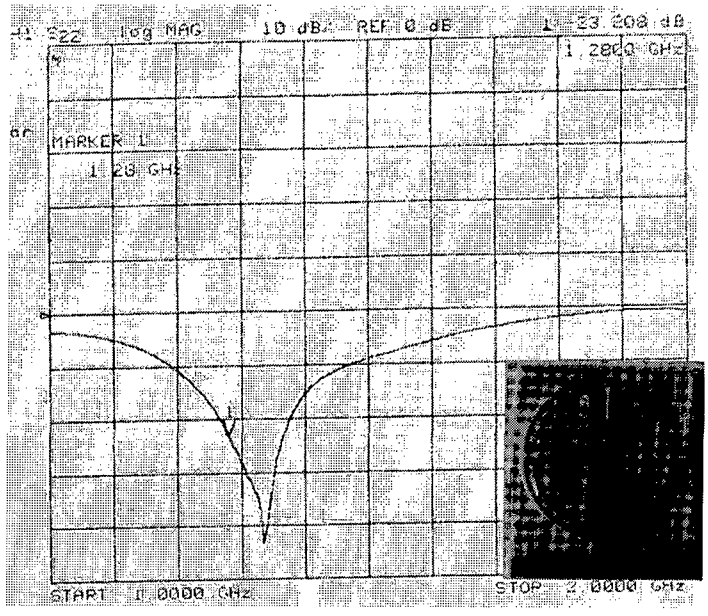

Figure 4.16: Fabricated antenna and measured return loss

The fabricated antenna was tested for its far-field radiation properties. Measurement were done for pattern in its both the planes (*E*-plane and *H*-plane power pattern).

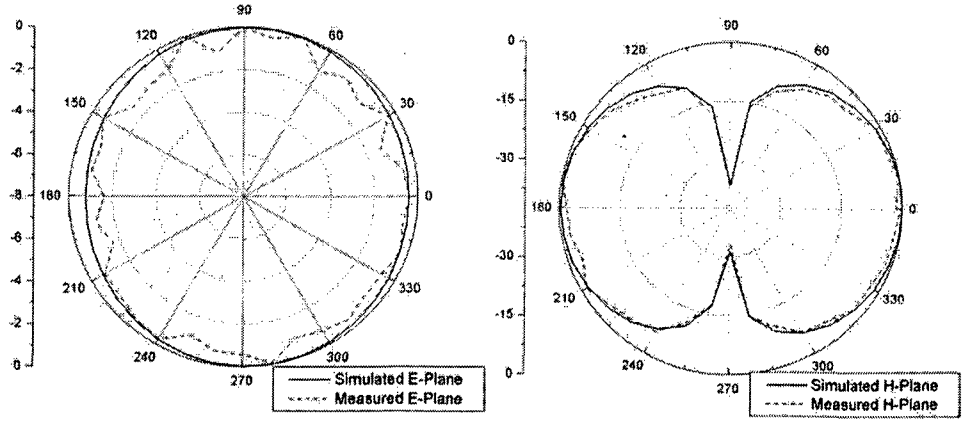

Figure 4.17 Simulated and Measured radiation pattern

Above Figure show the simulated and measured radiation patterns of the antenna in both the *E*-plane and the *H*-plane. These plots confirm the broadside directive radiation properties of the antenna. The simulated and measured radiation patterns are in close agreement except some ripples at the measured results. The measured radiation pattern in both *E*-plane and *H*-plane are somewhat distorted compared to that of simulated patterns. This may be due to the fact that low power levels are

received by the antenna. Possible reasons for these disagreements between simulated and measured results may due to the possible presence of interference and noise. The achieved impedance bandwidth (measured at -10 dB refection coefficient) is around 250MHz. The simulated gain was 2.1dBi.

So in this design size reduction of 81% have been achieved which is much more than the required (40%).

4.3 Design 2: Modified Split Ring Resonator for L-band (1.28 GHz) applications

A second a novel modified SRR is proposed for L-band (1.28 GHz) applications is proposed. An H-field coupling feed method is adopted with reduced ground plane. A notable size reduction of 81% in size is achieved with reasonable simulated gain.

4.3.1 Antenna Geometry and Parametric analysis

The proposed design is a slight modification of the previous resonator. The decoupled rings are joined together in this design to see the effect on performance. Fig.4.18 shows the schematic top and bottom view of the resonator. A detail parametric analysis is done to understand the resonance behavior and tuning of the antenna. It is observed that the resonance varies in an inverse relation to the radius of the inner ring where as in a proportional relation with the outer ring radius.

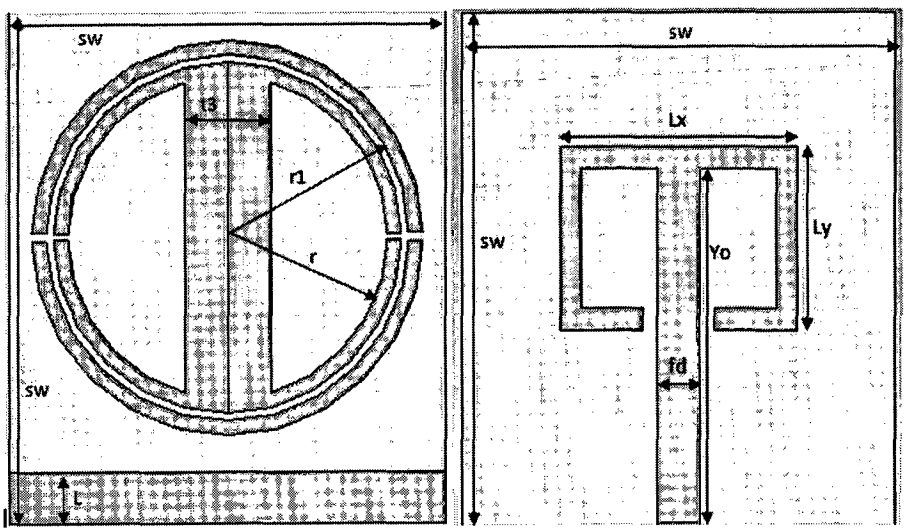

(a) (b)

Figure 4.18 (a) Top view (b) Bottom view of the resonator

Simulated return loss for above design is shown below in fig. 4.19. It can be observed from the figure that return loss is much less than -10 db (around -19 db) as is the requirement of the simulation.

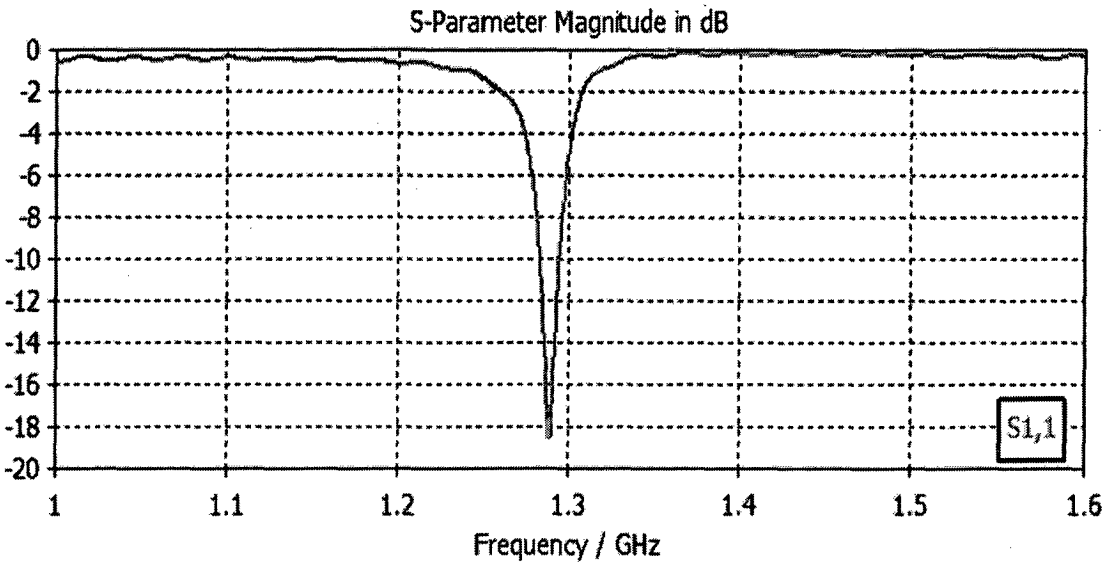

Figure 4.19 Simulated return loss

The microstrip feeding network and the resonator are in opposite sides of the dielectric substrate. As seen from the figure, the gap in the feeding network causes discontinuity in the electrical path. The changing electric current results magnetic flux loops. These changing magnetic flux when pass through the loops of the SRR, induces an electric current. Surface current distribution of the design is shown below in figure 4.20. The integrated inductance of transmission line and gap capacitance forms a resonator tank circuit operating at 1.28 GHz frequency.

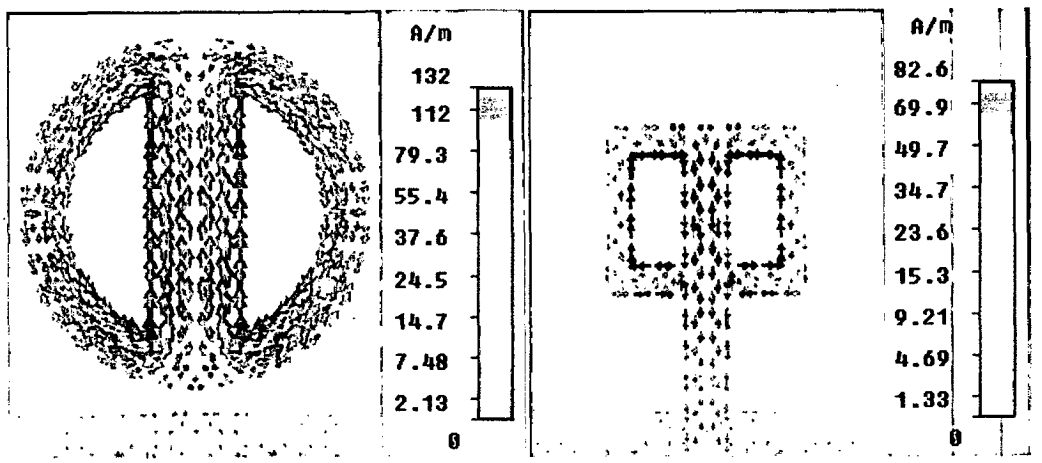

Figure 4.20 Surface current distributions at 1.28 GHz

The resonance can be easily tuned with a more number of degree of freedom modifying the design variables like inner ring radius (r), outer ring radius (r1) and gaps in rings (g & g1). A detail parametric analysis is done to understand the design. As we increase the outer radius (r1), the capacitance should decrease as the distance between two rings is increasing. As we know that the resonant frequency is inversely proportional to capacitance so on increasing r1 the resonant frequency should shift to right as shown in fig. 4.21 below.

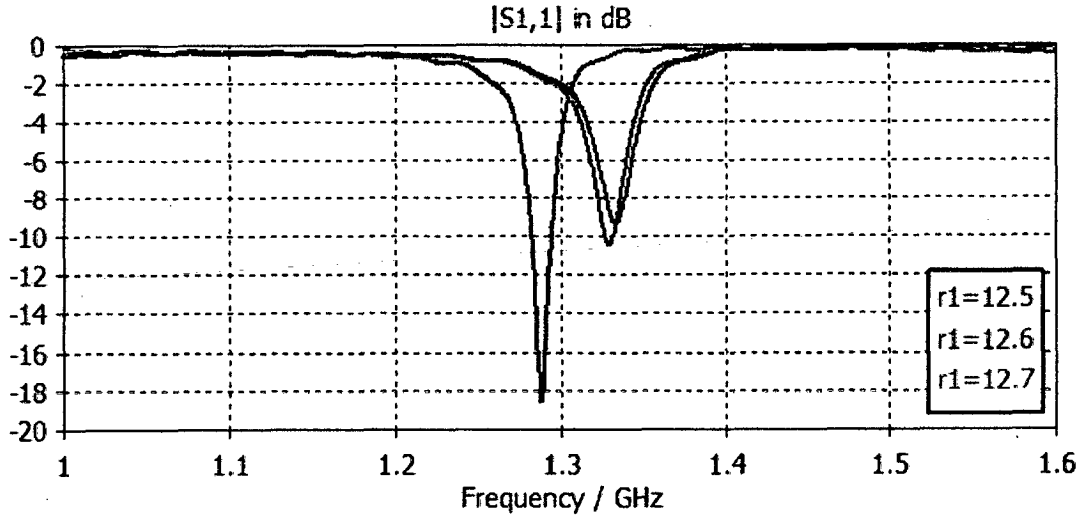

Figure 4.21 Variation of resonant frequency with outer ring radius (r1)

As we decrease the inner radius (r), the capacitance should decrease as the distance between two rings is increasing. As we know that the resonant frequency is inversely proportional to capacitance so on decreasing (r) the resonant frequency should shift to right as shown in fig. 4.22 below.

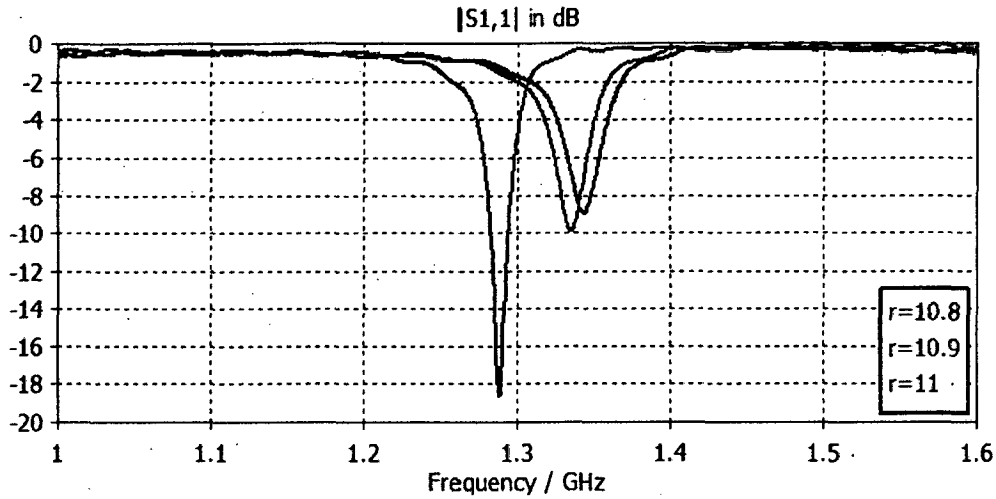

Figure 4.22 Variation of resonant frequency with inner ring radius (r)

As we increase the gaps in between the outer ring (g1) the capacitance decreases and there is right shift in resonant frequency as shown in the fig. 4.23 below.

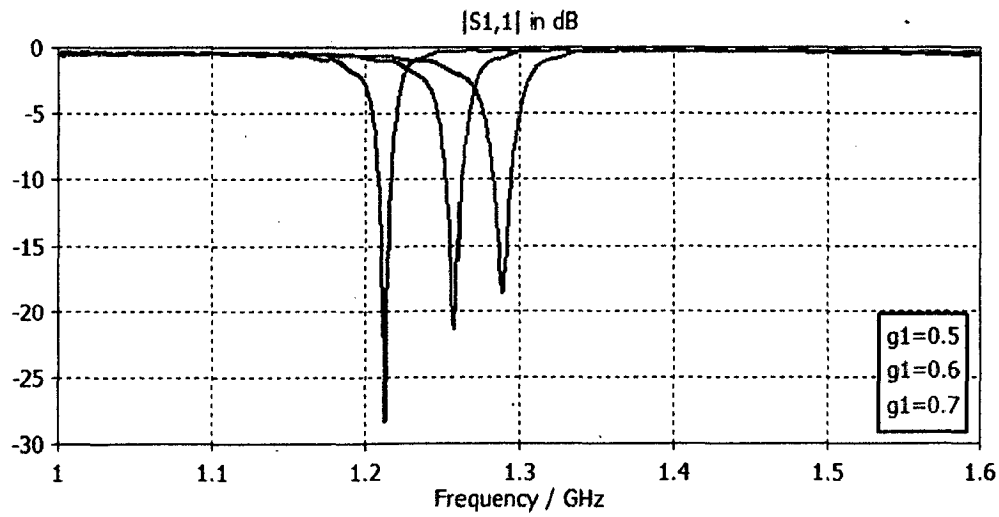

Figure 4.23 Variation of resonant frequency with outer ring gap (g1)

Similarly as we increase the gaps in between the inner ring (g) the capacitance decreases and there is right shift in resonant frequency as shown in the fig. 4.24 below.

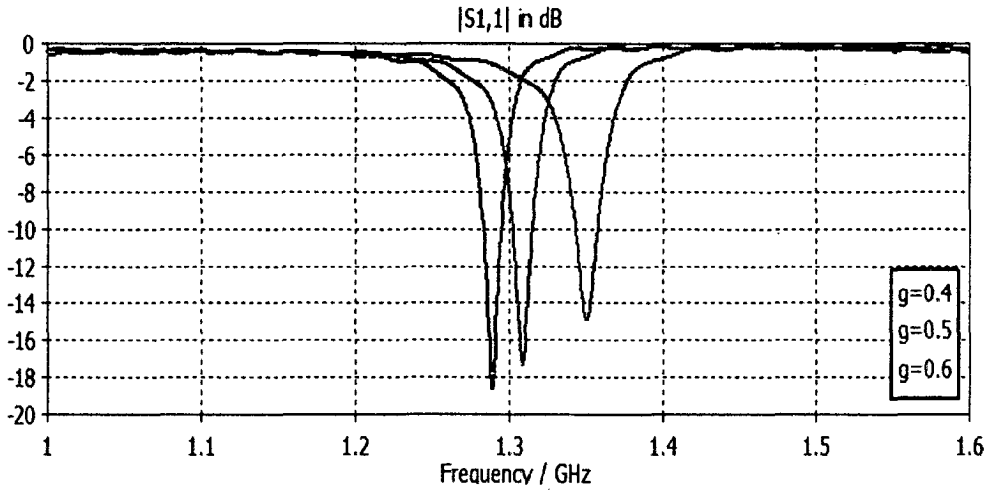

Figure 4.24Variation of resonant frequency with inner ring gap (g)

In this section we discussed the parameter sweep i.e. effect of varying various parameters of the given design on the resonant frequency of design. It has been shown that it shifts either right or left. In the next section we will discuss fabrication and measurement results.

4.3.2 Fabrication and Measurement Result

The proposed modified SRR after optimization and analysis was fabricated and tested in the laboratory. Fig. 4.25 shows the fabricated antenna and measured return loss being tested on HP network analyzer (HP 8720B). The radiation performance has been measured in the anechoic chamber keeping the fabricated prototype at receiver end. About 15dBm power was given to the transmitter antenna from the RF power generator, and the distance between the transmitter and the receiver was kept at 1.5 meter.

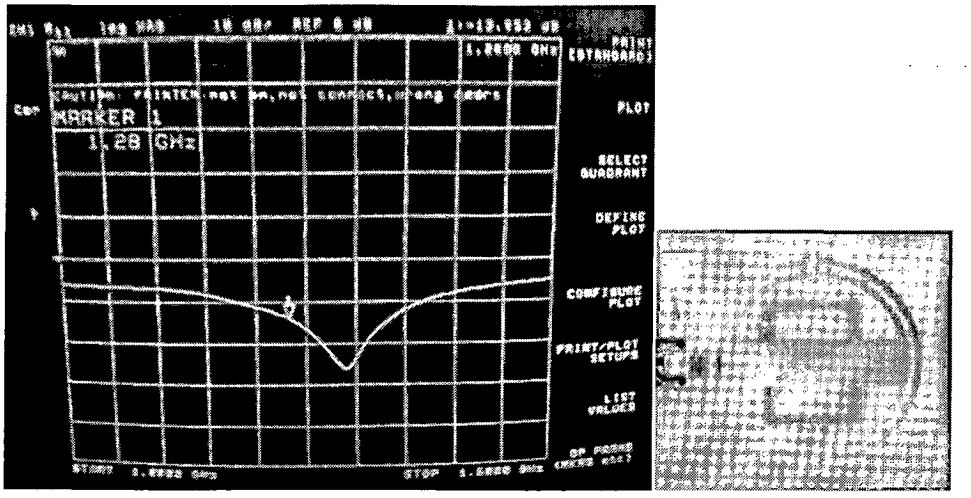

Figure 4.25Fabricated antenna and measured return loss

The fabricated antenna was test for its far-field radiation properties. Measurement were done for pattern in its both the planes (*E*-plane and *H*-plane power pattern).

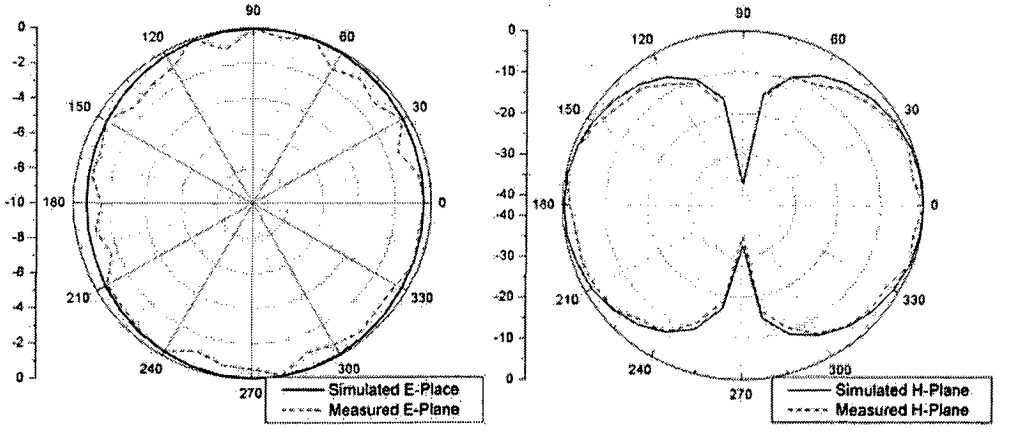

Figure 4.26 Simulated and Measured radiation pattern

Above figure show the simulated and measured radiation patterns of the antenna in both the *E*-plane and the *H*-plane. These plots confirm the broadside directive radiation properties of the antenna. The simulated and measured radiation patterns are in close agreement except some ripples at the measured results. The measured radiation pattern in both *E*-plane and *H*-plane are somewhat distorted compared to that of simulated patterns. This may be due to the fact that low power levels are received by the antenna. Possible reasons for these disagreements between simulated and measured results may due to the possible presence of interference and noise.

So in this design size reduction of 81% have been achieved which is much more than the required (40%).

4.4 Design 3: Modified Split Ring Resonator for L-band (1.28 GHz) applications

In the third design a modified SRR is proposed for L-band (1.28 GHz) applications is proposed. An H-field coupling feed method is adopted with reduced ground plane. A notable size reduction of 82% in size is achieved with reasonable simulated gain.

4.4.1 Antenna Geometry and Parametric analysis

The antenna configuration of the proposed resonator structure is shown in Fig. 4.27 with the dimensional notations. The gray color portion is the metallic part. The metallic resonator structure is on a commercially available low cost FR4 dielectric substrate with $\varepsilon_r = 4.4$, thickness of substrate is 1.524 mm with loss tangent 0.0024. A feed line of characteristic impedance as 50 Ω is adopted to feed the resonator. The width of the feed line (fd) was 2.8 mm to achieve 50 Ω. A square substrate of dimension 28 mm x 28 mm is used.

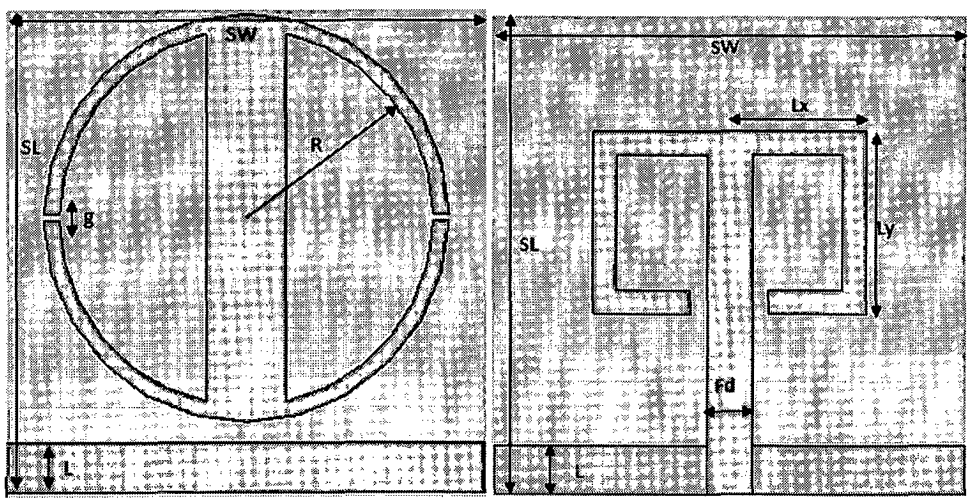

(a) (b)

Figure 4.27 (a) Top view (b) Bottom view of the proposed antenna

Simulated return loss for above design is shown below in fig. 4.28. It can be observed from the figure that return loss is much less than -10 db (around -27 db) as is the requirement of the simulation.

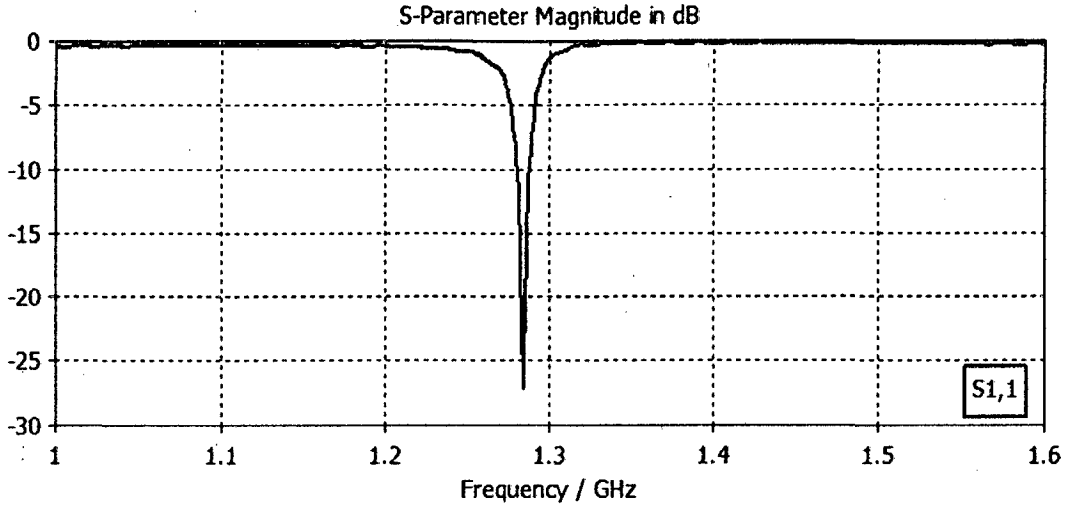

Figure 4.28 Simulated return loss of the antenna

The microstrip feeding network and the resonator are in opposite sides of the dielectric substrate. As seen from the figure, the gap in the feeding network causes discontinuity in the electrical path. The changing electric current results magnetic flux loops. These changing magnetic flux when pass through the loops of the SRR, induces an electric current. Surface current distribution of the design is shown below in figure 4.29. The integrated inductance of transmission line and gap capacitance forms a resonator tank circuit operating at 1.28 GHz frequency.

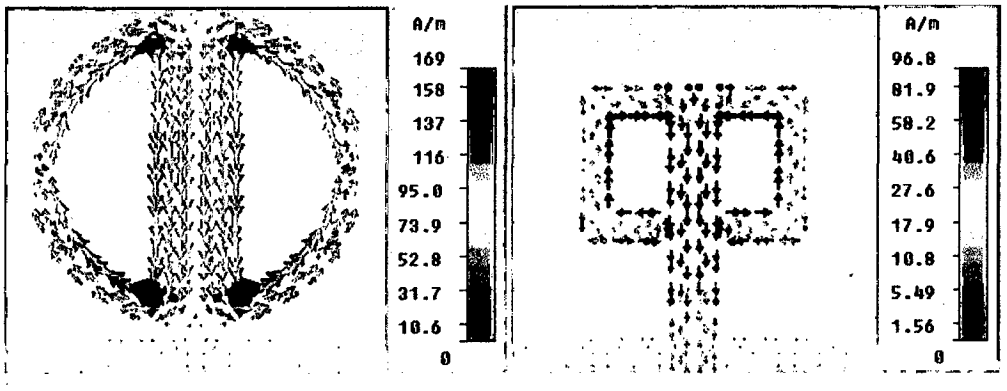

Figure 4.29 Surface current distributions at 1.28 GHz

As this is a single ring structure so when we increase the radius of the ring the physical length of structure increases so with that inductance of structure also increases. As we know that inductance is inversely proportional to the resonant frequency so on increasing the radius the resonant frequency shifts to left i.e. it decreases as shown in figure 4.30 below.

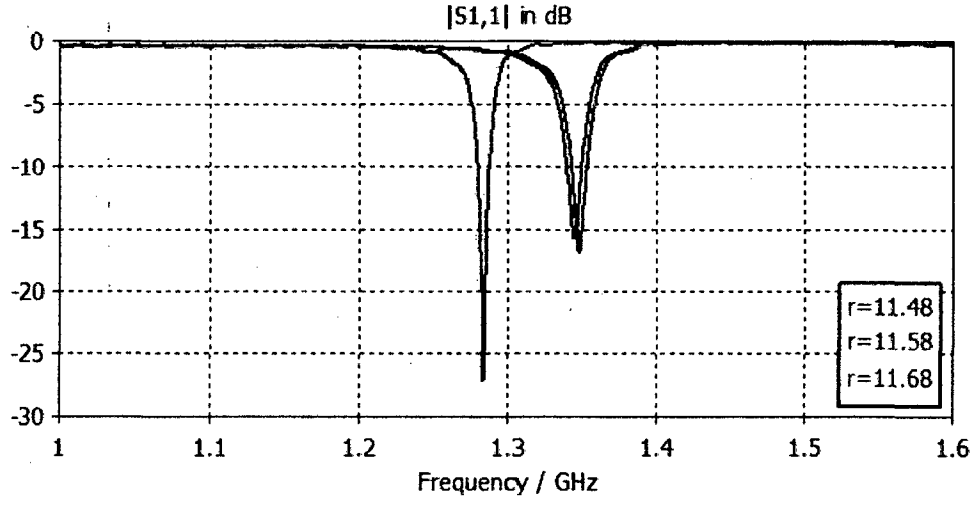

Figure 4.30Variation of resonant frequency with ring radius (R)

As we increase the gaps in between the ring (g) the capacitance decreases and there is right shift in resonant frequency as shown in the fig. 4.31 below.

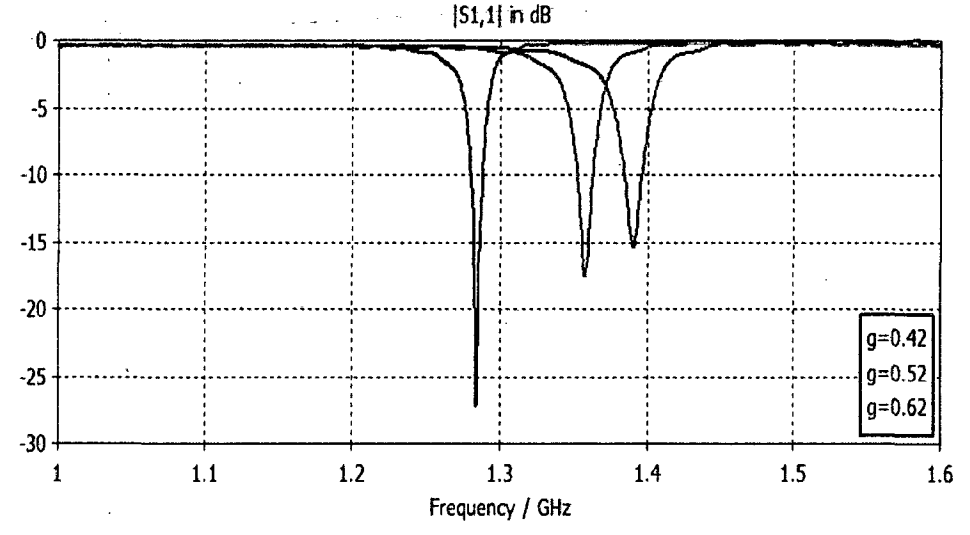

Figure 4.31Variation of resonant frequency with ring gap (g)

In this section we discussed the parameter sweep i.e. effect of varying various parameters of the given design on the resonant frequency of design. It has been shown that it shifts either right or left. In the next section we will discuss fabrication and measurement results.

4.4.2 Fabrication and Measurement Result

The proposed modified SRR after optimization and analysis was fabricated and tested in the laboratory. Fig. 4.32 shows the fabricated antenna and measured return loss being tested on HP network analyzer (HP 8720B). The radiation performance has been measured in the anechoic chamber keeping the fabricated prototype at receiver end. About 15dBm power was given to the transmitter antenna from the RF power generator, and the distance between the transmitter and the receiver was kept at 1.5 meter.

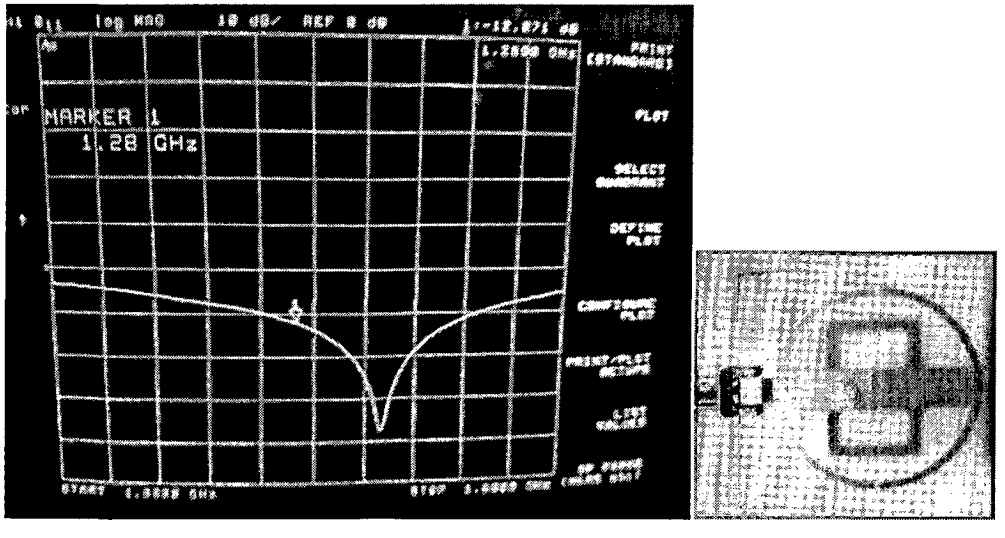

Figure 4.32Fabricated antenna and measured return loss

The fabricated antenna was test for its far-field radiation properties. Measurement were done for pattern in its both the planes (*E*-plane and *H*-plane power pattern).

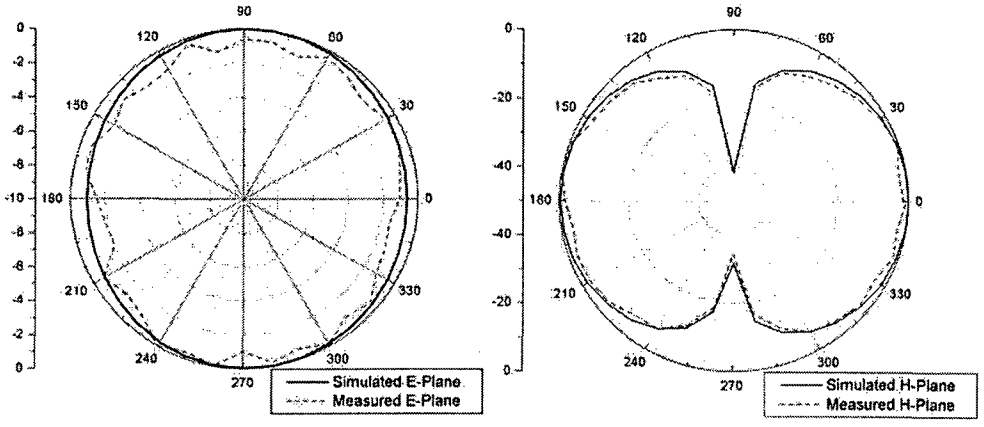

Figure 4.33 Simulated and Measured radiation pattern

Above figure show the simulated and measured radiation patterns of the antenna in both the *E*-plane and the *H*-plane. These plots confirm the broadside directive radiation properties of the antenna. The simulated and measured radiation patterns are in close agreement except some ripples at the measured results. The measured radiation pattern in both *E*-plane and *H*-plane are somewhat distorted compared to that of simulated patterns. This may be due to the fact that low power levels are received by the antenna. Possible reasons for these disagreements between simulated and measured results may due to the possible presence of interference and noise.

So in this design size reduction of 82% have been achieved which is much more than the required (40%).

4.5 Design 4: Modified Split Ring Resonator for L-band (1.28 GHz) applications

A forth modified version of the original SRR is proposed for L-band (1.28 GHz) applications. The feeding methodology is same as previous, i.e. H-field coupling

feed method is adopted with reduced ground plane. A notable size reduction of 82% in size is achieved with reasonable simulated gain.

4.5.1 Antenna Geometry and Parametric analysis

The antenna configuration of the proposed resonator structure is shown in Fig. 4.34 with the dimensional notations. The gray color portion is the metallic part. The metallic resonator structure is on a commercially available low cost FR4 dielectric substrate with $\varepsilon_r = 4.4$, thickness of substrate is 1.524 mm with loss tangent 0.0024. A feed line of characteristic impedance as 50 Ω is adopted to feed the resonator. The width of the feed line (fd) was 2.8 mm to achieve 50 Ω. A square substrate of dimension 28 mm x 28 mm is used. Typical return loss and surface current distribution is shown in Fig. 4.35 and Fig. 4.36 respectively. The length Sx provides extra capacitance. For proper impedance matching this has to be tuned accordingly.

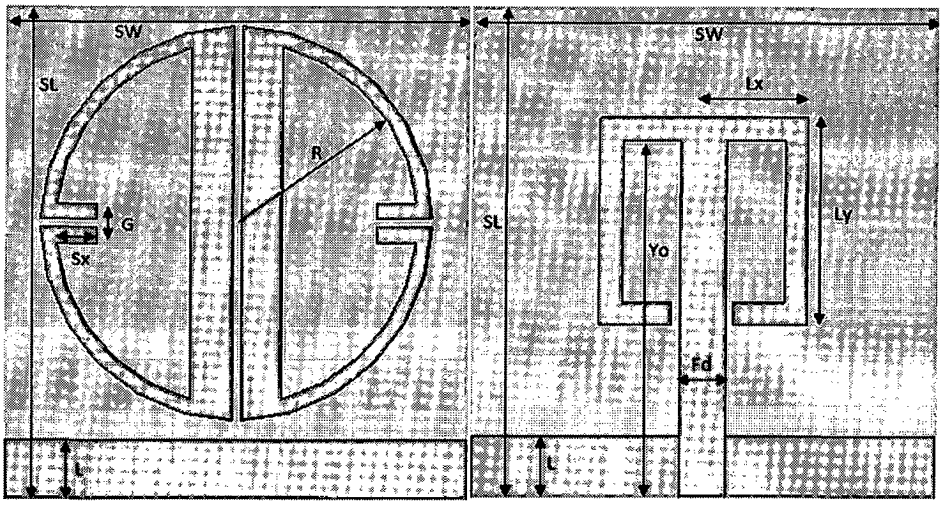

(a) (b)

Figure 4.34 (a) Top view (b) Bottom view

Simulated return loss for above design is shown below in fig. 4.35. It can be observed from the figure that return loss is much less than -10 db (around -35 db) as is the requirement of the simulation.

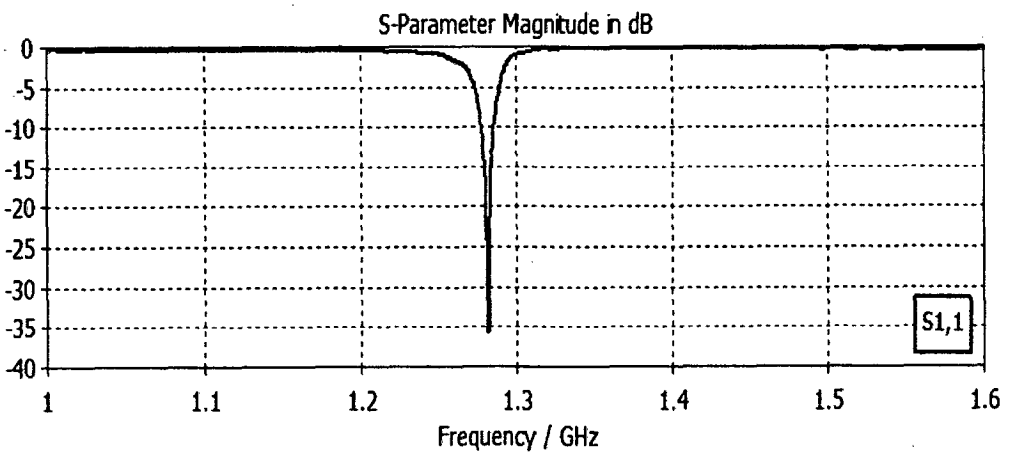

Figure 4.35 Simulated return loss

The microstrip feeding network and the resonator are in opposite sides of the dielectric substrate. As seen from the above figure, the gap of 1mm in the feeding network causes discontinuity in the electrical path. The changing electric current results magnetic flux loops. These changing magnetic flux when pass through the loops of the SRR, induces an electric current. Surface current distribution of the design is shown below in figure 4.36.

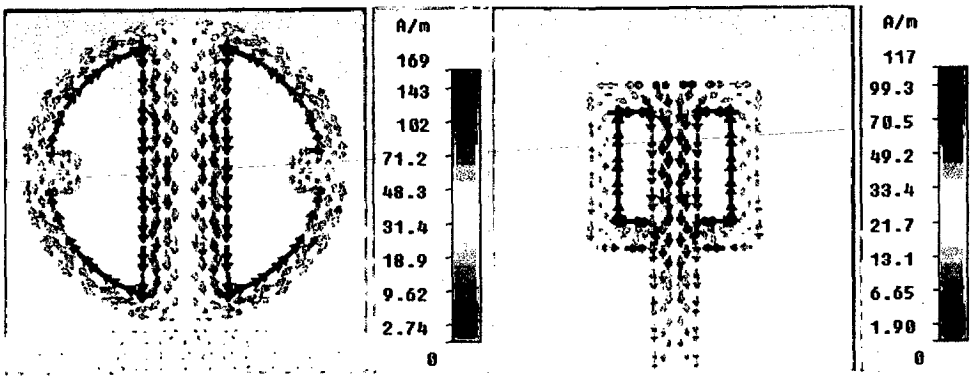

Figure 4.36 Surface current distributions at 1.28 GHz

The integrated inductance of transmission line and gap capacitance with capacitance due to S_x forms a resonator tank circuit operating at 1.28 GHz frequency. A detail parametric analysis is done to understand the design. On increasing the length S_x the inductance decreases and so the resonant frequency shifts to left i.e. it decreases as shown below in figure 4.37.

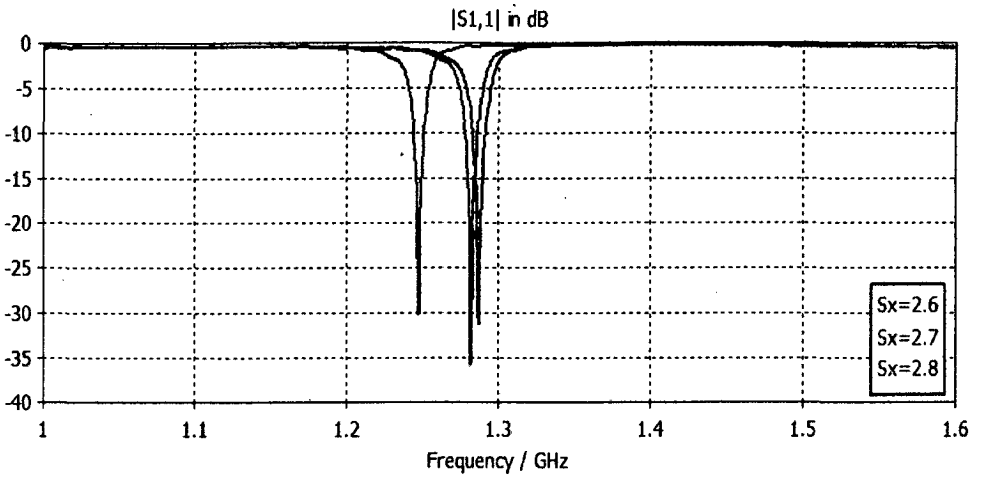

Figure 4.37Variation of resonant frequency with S_x

In this section we discussed the parameter sweep i.e. effect of varying various parameters of the given design on the resonant frequency of design. It has been shown that it shifts left on increasing S_x. In the next section we will discuss fabrication and measurement results.

4.5.2 Fabrication and Measurement Result

The proposed modified SRR after optimization and analysis was fabricated and tested in the laboratory. Fig. 4.25 shows the fabricated antenna and measured return loss being tested on HP network analyzer (HP 8720B). The radiation performance has been measured in the anechoic chamber keeping the fabricated prototype at receiver end. About 15dBm power was given to the transmitter antenna from the RF power generator, and the distance between the transmitter and the receiver was kept at 1.5 meter.

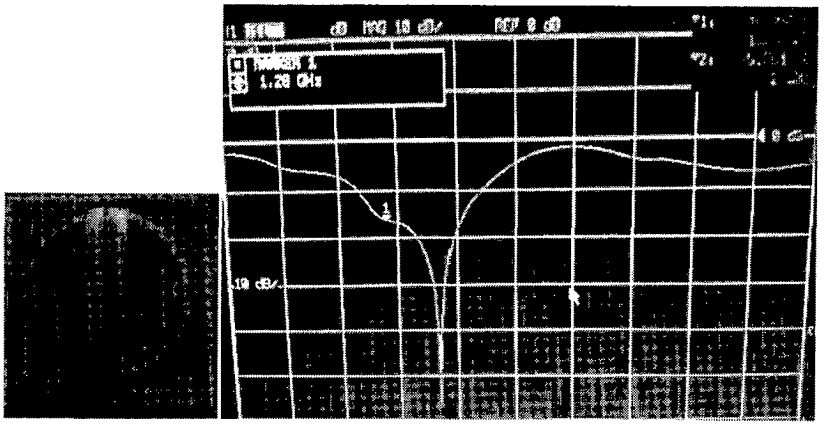

Figure 4.38Fabricated antenna and measured return loss

The fabricated antenna was test for its far-field radiation properties. Measurement were done for pattern in its both the planes (*E*-plane and *H*-plane power pattern)

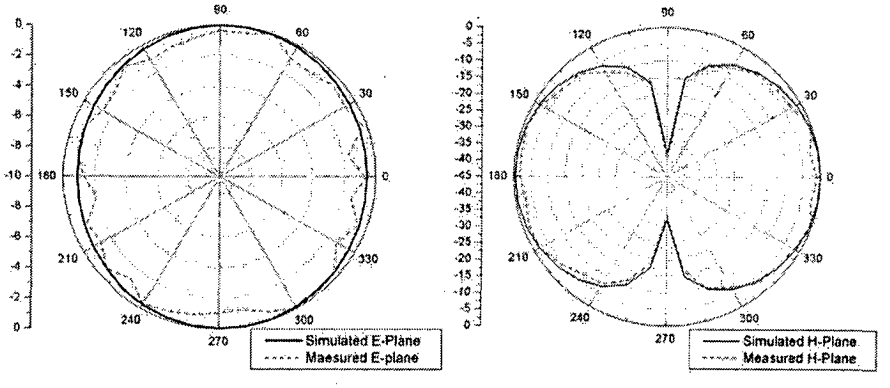

Figure 4.39 Simulated and Measured radiation pattern

Above figure show the simulated and measured radiation patterns of the antenna in both the *E*-plane and the *H*-plane. These plots confirm the broadside directive radiation properties of the antenna. The simulated and measured radiation patterns are in close agreement except some ripples at the measured results. The measured radiation pattern in both *E*-plane and *H*-plane are somewhat distorted compared to that of simulated patterns. This may be due to the fact that low power levels are received by the antenna. Possible reasons for these disagreements between simulated and measured results may due to the possible presence of interference and noise. So in this design size reduction of 82% have been achieved which is much more than the required (40%).

Chapter 5
Conclusions and Future Scope

5.1 Conclusion

The overall work done can be presented briefly as follows. In the first part of the report, a detail study of the microstrip patch antenna and Various Metamaterials structures has been done. Different structures having specific properties of LH nature, i.e. either negative permittivity or negative permeability or both are studied. The planner Metamaterials and composite right left Metamaterials has been studied. The effective parameter extraction of these materials at the band of interest has been studied. The underlying principles are discussed.

In the second part, a detail literature survey has been done on patch antenna and Metamaterials. The various applications of Metamaterials to microstrip patch antennas for performance enhancement and in specific size reduction has been done. Performance like directivity, gain, and return loss enhancement can be achieved using various Metamaterials structure.

In third chapter, the design methodology has been discussed. The simulation of SRR for effective parameter extraction has been discussed. The simulation set up and different boundary conditions to excite Left Handed nature of Metamaterials are discussed.

In the forth chapter, the simulation and design analysis of the main proposed Metamaterial inspired modified split ring resonator for L-band (1.28 GHz) application is presented. A detail parametric analysis has been done to explain frequency tuning of the antenna. A number of variations of the main design have also been studied to fully characterize its operation and performance in terms of band width, maximum realizable gain and resonance frequency tuning capability. All the designs are fabricated and characterized in the laboratory in terms of return loss and radiation pattern in both the plane.

5.2 Scope of future work

With the proposed design during the dissertation, a notable size reduction of around 80% has been achieved at L-band 1.28 GHz. A further investigation can be made to reduce its physical size even more. Other modifications of the proposed design can be tried for miniaturization. Different feeding with different topologies of resonant Metamaterial may be tried for better performance, gain with size reduction.

Publication(s)

1. Davinder Singh, Jagannath Malik, Amalendu Patnaik and M.V. Kartikeyan, *Senior Member IEEE, "Novel Modified SRR with H-field Coupled feed for L-band (1.28 GHz) Remote Sensing Applications,"* National conference on Recent Trends on Microwave techniques and applications, Jaipur, 2012 India.

2. Davinder Singh, Jagannath Malik, Amalendu Patnaik, "*Metamaterial Inspired Compact L-Band antenna for Remote Sensing Application*" (in review).

References

[1] Christophe Caloz, Tatsuo Itoh, "*Electromagnetic Metamaterials: Transmission Line Theory and Microwave Applications*", Johan Wiley, New Jersey, 2006.

[2] Lukcsjelinek, Jan Machac, Jdnzehentner," *Metamaterials - A Challenge for ContemporaryAdvanced Technology*", *IEEE,* 2007.

[3] J. B. Pendry, A. J. Holden, D. J. Robbins and W. J. Stewart, "*Magnetism from conductors and enhanced nonlinear phenomena*", *IEEE Trans. Microwave Theory Tech.*, vol. 47, no.11, pp. 2075-2084, Nov. 1999.

[4] H. Cori and C. Zach," *Wave Propagation in metamaterial multi-layered structures*", Microwave and Optical Technology Letters, vol. 3 (6), pp.460-465 ,2004.

[5] N. Engheta, "*A idea for thin sub wavelength cavity resonators using metamaterials with negative permittivity and permeability*", *IEEE Antennas and Wireless Propagation Letters*, vol. 1 no. 1, pp. 10-13, 2002.

[6] Alu and N. Engheta,. "*Guided nodes in a waveguide filled with a pair of Single-Negative (SNG), Double-Negative (DNG), and/or Double-Positive (DPS) layers*" *IEEE Trans. Microwave Theory Tech.*, vol. 52, pp. 199-210, Jan. 2004.

[7] J. B. Pendry, "*Negative refraction makes a perfect lens*" *Phys. Rev. Lett.*, vol.85, pp. 3966-3969, oct. 2000.

[8] Grbic and G. V. Eleftheriades, "*Experimental verification of backward-wave radiation from a negative refractive index metamaterial*", *J. Appl. Phys.*, vol.92, pp. 5930-5935, Nov. 2002.

[9] Omar F., Siddiqui; Mo Mojahedi, George V. Eleftheriades "*Periodically LTL with Effective NRI and Negative Group Velocity*", IEEE *Transactions on Antennas and Propagation,* vol. 1 no. 10, pp 2619–2625. Oct 2003.

[10] Huangfu, J., L. Ran, H. Chen, X. Zhang, K. Chen, T. M. Grzegorczyk, and J. A. Kong, "*Experimental confirmation of negative refractive index of metamaterial composed of W-like Metallic patterns*," Applied Physics Lett., Vol. 84, No. 9, 2004.

[11] LukcsJelinek, Jan Machac, JdnZehentner, "*Metamaterials - A Challenge for Contemporary Advanced Technology*" ,*IEEE*, 2007.

[12] A.K. Iyer, G. V. Eleftheriades, "*Negative refractive index metamaterials supporting 2-D waves*", *IEEE MTT-S International Microwave Symposium Digest*, vol. 2, pp. 1067-1070, June 2002.

[13] G. V. Eleftheriades, A. K. Iyer, P. C. Kremer, "*Planar negative refractive index media using periodically L-C loaded transmission lines*," *IEEE Trans. on Microwave Theory and Tech.*, vol. 50, no. 12, pp. 2702-2712, Dec.2002.

[14] A. K. Iyer, P. C. Kremer, and G. V. Eleftheriades, "*Experimental and theoretical verification of focusing in a large, periodically loaded transmission line negative refractive index metamaterial*," *Optics Express*, vol. 11, pp. 696-708, 2003.

[15] G.V. Eleftheriades, "*Negative-Refractive-Index Transmission-Line metamaterials and Enabling Microwave Devices*,", *Radio Science Bulletin No 312*, pp. 57-69, March 2005.

[16] O"Brien, S. and J. B. Pendry, "*Magnetic activity at infrared frequencies in structured metallic photoniccrystals*," Journal on Phys: Condens .Matter 14, pp. 6383–6394, 2002.

[17] Smith, D. R., W. J. Padilla, D. C. Vier, S. C. Nemat-Nasser, and S. Schultz, "*Composite medium with simultaneously negative*" , Phys. Rev. Lett.,84, 4184, 2000.

[18] Huangfu, J., L. Ran, H. Chen, X. Zhang, K. Chen, T. M. Grzegorczyk, and J. A. Kong, "*Experimental confirmation of negative refractive index of metamaterial composed of W-like Metallic patterns*," Applied Physics Lett., Vol. 84, No. 9, 2004.

[19] Chen, H., L. Ran, J. Huangfu, X. Zhang, K. Chen, T. M. Grzegorczyk, and J. A. Kong, "*Left-handed material composed of only S-shaped resonators*," Progress In Electromagnetics Research, vol 51, pp 249–279, 2005.

[20] G. A. Deschamps"Microstrip *Microwave Antennas*,"*3rd USAF Symp. On Antenna*, 1953.

[21] R. E. Munson, 3*Single slot cavity antennas assembly*,in*U.S. Patent No. 3713162*, Jan. 23, 1973.

[22] C. A. Balanis , "*Antenna Theory : Analysis and design, chapter- Microstrip antenna*" *John Wiley and Sons, Inc., Singapore*, 2002.

[23] K. L. Wong, "*Compact and Broadband Microstrip Antennas, John Wiley and Sons, Inc., New York*, 2002.

[24] E. R. Iglesias, O. Q. Teruel and L. I. S. Sanchez"*Mutual coupling reduction in patch antenna arrays by using a planar EBG structure & a multilayer dielectric substrate*" *IEEE Transactions Antennas and Propagation*,vol. 56, no. 6, pp. 1648-55, June 2008.

[25] S. Enoch, "*A metamaterial directive emission,t,Physical Review Letters*, vol. 21, pp. 1-4, Nov. 2002.

[26] Q. Wu, P. Pan,F. Y. Meng, L. W. li and J. Wu, , "*A novel flat lens antenna design based on zero refraction principle metamaterial,*"e*Journal of Applied Physics*, vol. 87, pp. 151-156, 2007.

[27] F. Yang and Y. R. Samii, "*Reflection phase characterization of the EBG ground plane for low profile wire antenna applications*,ro*EEE Antennas and Wireless Propagation Letters*, vol. 51, pp. 2691-2703, Oct. 2003.

[28] C. J. Lee, K. M. K. H. Leong and T. Itoch, K. M. K. H. Leon antenna using composite right/left handed transmission line, *Antennas and propagation international symposium*, 2005.

[29] K. Buell, H. Mosallaei and K. Sarbandi, "*A substrate for small patch antennas, providing tunable miniaturization factors*" *IEEE Transactions on Microwave Theory and Techniques*, vol. 54, no. 1, pp. 135-144, January 2006.

[30] Ahmad A. Sulaiman, Ahmad S. Nasaruddin, Mohd H. Jusoh, Nor H. Baba, Rabi'atun A. Awang, Mohd F. Ain, "*Bandwidth Enhancement in Patch Antenna by Metamaterial Substrate*" European Journal of Scientific Research ISSN 1450-216X Vol.44 No.3 , pp.493-501, 2010.

[31] Ahmad A. Sulaiman, Mohamad Z. M. Zani, Mohd H. Jusoh, Noor H. Baba, Robi'atun A. Awang, Mohd F. Ain, "*Circular Patch Antenna on Metamaterial*" European Journal of Scientific Research, Vol.45 No.3, pp.391-399, 2010.

[32] IrajArghandLafmajani, PejmanRezaei, "*Miniaturized Rectangular Patch Antenna Loaded with Spiral/Wires Metamaterial*" European Journal of Scientific Research Vol.65 No.1, pp. 121-130, 2011.

[33] Yoonjae Lee, Yang Hao, "Characterization of microstrip patch antennas on metamaterial substrates loaded with complementary split-ring resonators" microwave and optical technology letters / Vol. 50, No. 8, August 2008.